with resistances of 2–4 MΩ. Currents were digitized with the Digidata 1322A and 1440A data acquisition systems (Axon Instruments, Molecular Devices Inc.). Data were captured using PClamp 8.1 & 10 software and analysed using ClampFit 10.2 (Axon Instruments). Currents were low-pass filtered at 5 kHz and sampled at 10 kHz. Capacity transients were cancelled, however, series resistance were not compensated. Voltages were not corrected for liquid junction potentials. Recordings were performed at room temperature. Recordings were carried out in the perforated patch configuration. The pipette solution contained (in mM) 110 CH_3COOK, 30 KCl, 5 NaCl, 1 $MgCl_2$ and 10 HEPES (pH corrected to 7.35 using KOH, osmolarity: ~310 mOsm with sucrose). 205 Mg per mililitre of fresh amphotericin B was added to this solution before recording. The bath solution contained (in mM): 140 NaCl, 4 KCl, 2 $CaCl_2$, 1 $MgCl_2$, 5 glucose and 10 HEPES (pH 7.4 adjusted using NaOH, osmolarity: ~320 mOsm with sucrose). 8-pCPT was added to the bath solution after establishment of a stable response to a 0.008 Hz mechanical stimulus. In HEK293 cells expressing Piezo1/2 either bath solution or 8-pCPT was added to the bath solution. Recordings were made 20–50 min after the addition of 8-pCPT at room temperature. For experiments in which cytosolic Ca^{2+} concentration was fixed, the conventional whole-cell configuration was used. Whole-cell patch clamp solution contained (in mM) KCl (130), $MgCl_2$ (2.5), $CaCl_2$ (1.94 or 4.63 to give 50 nM or 1 μM free Ca^{2+}), EGTA (5) K-ATP (3) HEPES (5) and pH 7.4 KOH (osmolarity was set to 310 mOsm with sucrose).

Mechanical stimulation. Mechanical stimulation of cell bodies was achieved using a heat-polished glass pipette (tip diameter ~2 μm), controlled by a piezo-electric crystal drive (Siskiyou MXPZT-300 series or Burleigh LSS-3000 series), positioned at an angle of about 70° to the surface of the dish. The probe was positioned so that a ~x μm (x = 10–14 μm) movement did not visibly contact the cell but that a x + 1 μm stimulus produced an observable membrane deflection. The probe was moved at a speed of 1 μm ms^{-1} and the stimulus was applied for 250 ms. A series of mechanical steps in ~1 (HEK cells) or ~2 μm (DRG neurons) increments were applied. Criteria for classifying adaptation kinetics of rapidly adapting mechanosensitive currents (RA) in DRG neurons had a decay kinetic that was best described by a bi-exponential fit[5]. Kinetics of adaptation to the mechanical stimuli were fitted with a standard mono exponential decay with the equation below using PClamp 10.2.

$$f(t) = \sum_{i=1}^{n} A_i e^{-t/\tau_i} + C$$

The fit solves for the amplitude A, the time constant τ, and the constant y-offset C for each component i.

Western blot analysis. DRG cultures were homogenized in ice-cold RAL lysis buffer (200 mM NaCl, 50 mM Tris–HCl (pH 7.5), 10% glycerol, 1% NP-40, 2 mM sodium orthovanadate, 2 mM phenylmethylsulfonyl fluoride and protease inhibitor mix (Sigma-Aldrich, p3840, 1:100)). Proteins were separated by SDS–polyacrylamide gel electrophoresis and transferred to PVDF membranes (Millipore, Bedford, MA, USA). Blots were stained with mouse-anti-Epac1 and as loading control rabbit-anti-β-actin or the neuron-specific mouse-anti-β3-tubulin (all cell signalling). Subsequently, blots were incubated with goat anti-mouse-peroxidase or donkey-anti-rabbit IgG + IgM (H + L) (GE Healthcare) and developed by enhanced chemiluminescence plus (Amersham Int.).

mRNA isolation and real-time PCR. Lumbar DRGs (L2-L5) were isolated and total RNA was isolated with RNeasy Mini Kit (Qiagen) in accordance with the manufacturer's instructions. Reverse transcription was performed with 1 μg of RNA by using iScript Select cDNA Synthesis Kit (Invitrogen). Real-time quantitative PCR was then performed with iQ SYBR Green Supermix (Invitrogen). The following primer pairs were used:

Epac1: 5′-gTgTTggTgAAggTCAATTCTg-3′ (forward), 5′-CCACACCACgggCATC-3′ (reverse)

Epac2: 5′-TgTTAAAgTgTCTgAgACCAgCA-3′ (forward), 5′-AAAggCTgTCCCAATTCCCAg-3′ (reverse)

Piezo1: 5′-CTACAAATTCgggCTggAg-3′ (forward), 5′-TCCAgCgCCATggATAgT-3′ (reverse)

Piezo2: 5′-CCAAgTAgCCCATgCAAAAT-3′ (forward), 5′-gCATAACCCTgTgCCAgATT-3′ (reverse)

β-Actin: 5′-AgAgggAAATCgTgCgTgAC-3′ (forward), 5′-CAATAgTgATgACCTggCCgT-3′ (reverse)

GAPDH: 5′-TgAAgCAggCATCTgAgg-3′ (forward), 5′-CgAAggTggAAgAgTgggAg-3′ (reverse)

Data analysis. Data are expressed as mean ± s.e.m. Measurements were compared using Student's t-test, one-way one-way analysis of variance (ANOVA), repeated measures, or two-way ANOVA followed by Bonferroni's analysis. A P-value of <0.05 was considered to be statistically significant.

References

1. Di Castro, A., Drew, L. J., Wood, J. N. & Cesare, P. Modulation of sensory neuron mechanotransduction by PKC- and nerve growth factor-dependent pathways. *Proc. Natl Acad. Sci. USA* **103,** 4699–4704 (2006).
2. Wood, J. N. & Eijkelkamp, N. Noxious mechanosensation-molecules and circuits. *Curr. Opin. Pharmacol.* **12,** 4–8 (2012).
3. Costigan, M., Scholz, J. & Woolf, C. J. Neuropathic pain: a maladaptive response of the nervous system to damage. *Annu. Rev Neurosci.* **32,** 1–32 (2009).
4. Coste, B. *et al.* Piezo1 and Piezo2 are essential components of distinct mechanically activated cation channels. *Science* **330,** 55–60 (2010).
5. Quick, K. *et al.* TRPC3 and TRPC6 are essential for normal mechanotransduction in subsets of sensory neurons and cochlear hair cells. *Open. Biol.* **2,** 120068 (2012).
6. Hucho, T. & Levine, J. D. Signaling pathways in sensitization: toward a nociceptor cell biology. *Neuron* **55,** 365–376 (2007).
7. Bos, J. L. Epac proteins: multi-purpose cAMP targets. *Trends Biochem. Sci.* **31,** 680–686 (2006).
8. Wei, F. *et al.* Genetic elimination of behavioral sensitization in mice lacking calmodulin-stimulated adenylyl cyclases. *Neuron* **36,** 713–726 (2002).
9. Pierre, S., Eschenhagen, T., Geisslinger, G. & Scholich, K. Capturing adenylyl cyclases as potential drug targets. *Nat. Rev. Drug Discov.* **8,** 321–335 (2009).
10. Yajima, Y. *et al.* Differential involvement of spinal protein kinase C and protein kinase A in neuropathic and inflammatory pain in mice. *Brain Res.* **992,** 288–293 (2003).
11. Malmberg, A. B. *et al.* Diminished inflammation and nociceptive pain with preservation of neuropathic pain in mice with a targeted mutation of the type I regulatory subunit of cAMP-dependent protein kinase. *J. Neurosci.* **17,** 7462–7470 (1997).
12. Grandoch, M., Roscioni, S. S. & Schmidt, M. The role of Epac proteins, novel cAMP mediators, in the regulation of immune, lung and neuronal function. *Br. J. Pharmacol.* **159,** 265–284 (2010).
13. Gloerich, M. & Bos, J. L. Epac: defining a new mechanism for cAMP action. *Annu. Rev. Pharmacol. Toxicol.* **50,** 355–375 (2010).
14. Holz, G. G., Kang, G., Harbeck, M., Roe, M. W. & Chepurny, O. G. Cell physiology of cAMP sensor Epac. *J. Physiol.* **577,** 5–15 (2006).
15. McCarter, G. C., Reichling, D. B. & Levine, J. D. Mechanical transduction by rat dorsal root ganglion neurons *in vitro*. *Neurosci. Lett.* **273,** 179–182 (1999).
16. Drew, L. J., Wood, J. N. & Cesare, P. Distinct mechanosensitive properties of capsaicin-sensitive and -insensitive sensory neurons. *J. Neurosci.* **22,** RC228 (2002).
17. Drew, L. J. *et al.* Acid-sensing ion channels ASIC2 and ASIC3 do not contribute to mechanically activated currents in mammalian sensory neurones. *J. Physiol.* **556,** 691–710 (2004).
18. Hu, J. & Lewin, G. R. Mechanosensitive currents in the neurites of cultured mouse sensory neurones. *J. Physiol.* **577,** 815–828 (2006).
19. Hao, J. & Delmas, P. Multiple desensitization mechanisms of mechanotransducer channels shape firing of mechanosensory neurons. *J. Neurosci.* **30,** 13384–13395 (2010).
20. Drew, L. J. & Wood, J. N. FM1-43 is a permeant blocker of mechanosensitive ion channels in sensory neurons and inhibits behavioural responses to mechanical stimuli. *Mol. Pain* **3,** 1 (2007).
21. Kimitsuki, T. & Ohmori, H. Dihydrostreptomycin modifies adaptation and blocks the mechano-electric transducer in chick cochlear hair cells. *Brain Res.* **624,** 143–150 (1993).
22. Cho, H., Shin, J., Shin, C. Y., Lee, S. Y. & Oh, U. Mechanosensitive ion channels in cultured sensory neurons of neonatal rats. *J. Neurosci.* **22,** 1238–1247 (2002).
23. Hucho, T. B., Dina, O. A. & Levine, J. D. Epac mediates a cAMP-to-PKC signaling in inflammatory pain: an isolectin B4(+) neuron-specific mechanism. *J. Neurosci.* **25,** 6119–6126 (2005).
24. Abrahamsen, B. *et al.* The cell and molecular basis of mechanical, cold, and inflammatory pain. *Science* **321,** 702–705 (2008).
25. Ferrari, L. F., Chum, A., Bogen, O., Reichling, D. B. & Levine, J. D. Role of Drp1, a key mitochondrial fission protein, in neuropathic pain. *J. Neurosci.* **31,** 11404–11410 (2011).
26. Eijkelkamp, N. *et al.* Low nociceptor GRK2 prolongs prostaglandin E2 hyperalgesia via biased cAMP signaling to Epac/Rap1, protein kinase C{varepsilon}, and MEK/ERK. *J. Neurosci.* **30,** 12806–12815 (2010).
27. Djouhri, L. & Lawson, S. N. Abeta-fiber nociceptive primary afferent neurons: a review of incidence and properties in relation to other afferent A-fiber neurons in mammals. *Brain Res. Brain Res. Rev.* **46,** 131–145 (2004).
28. Zhu, Y. F. & Henry, J. L. Excitability of abeta sensory neurons is altered in an animal model of peripheral neuropathy. *BMC Neurosci.* **13,** 15 (2012).
29. Oestreich, E. A. *et al.* Epac and phospholipase cepsilon regulate Ca2+ release in the heart by activation of protein kinase cepsilon and calcium-calmodulin kinase II. *J. Biol. Chem.* **284,** 1514–1522 (2009).

30. Kim, S. E., Coste, B., Chadha, A., Cook, B. & Patapoutian, A. The role of *Drosophila* piezo in mechanical nociception. *Nature* **19,** 209–212 (2012).
31. Suzuki, S. *et al.* Differential roles of Epac in regulating cell death in neuronal and myocardial cells. *J. Biol. Chem.* **285,** 24248–24259 (2010).
32. Akopian, A. N. *et al.* The tetrodotoxin-resistant sodium channel SNS has a specialized function in pain pathways. *Nat. Neurosci.* **2,** 541–548 (1999).
33. Ostman, J. A., Nassar, M. A., Wood, J. N. & Baker, M. D. GTP up-regulated persistent Na+ current and enhanced nociceptor excitability require NaV1.9. *J. Physiol.* **586,** 1077–1087 (2008).
34. Minett, M. S. *et al.* Distinct Nav1.7-dependent pain sensations require different sets of sensory and sympathetic neurons. *Nat. Commun* **24,** 791 (2012).
35. Hargreaves, K., Dubner, R., Brown, F., Flores, C. & Joris, J. A new and sensitive method for measuring thermal nociception in cutaneous hyperalgesia. *Pain* **32,** 77–88 (1988).
36. Chaplan, S. R., Bach, F. W., Pogrel, J. W., Chung, J. M. & Yaksh, T. L. Quantitative assessment of tactile allodynia in the rat paw. *J. Neurosci. Methods* **53,** 55–63 (1994).
37. Minett, M. S. *et al.* Distinct Nav1.7-dependent pain sensations require different sets of sensory and sympathetic neurons. *Nat. Commun.* **3,** 791 (2012).
38. Lai, J. *et al.* Immunofluorescence analysis of antisense oligodeoxynucleotide-mediated 'knock-down' of the mouse delta opioid receptor *in vitro* and *in vivo*. *Neurosci. Lett.* **213,** 205–208 (1996).
39. Hylden, J. L. & Wilcox, G. L. Intrathecal morphine in mice: a new technique. *Eur. J. Pharmacol.* **67,** 313–316 (1980).
40. Mabuchi, T. *et al.* Pituitary adenylate cyclase-activating polypeptide is required for the development of spinal sensitization and induction of neuropathic pain. *J. Neurosci.* **24,** 7283–7291 (2004).
41. Bennett, G. J. & Xie, Y. K. A peripheral mononeuropathy in rat that produces disorders of pain sensation like those seen in man. *Pain* **33,** 87–107 (1988).
42. Dickenson, A. H. & Sullivan, A. F. Electrophysiological studies on the effects of intrathecal morphine on nociceptive neurones in the rat dorsal horn. *Pain* **24,** 211–222 (1986).
43. Shpacovitch, V. M. *et al.* Agonists of proteinase-activated receptor-2 modulate human neutrophil cytokine secretion, expression of cell adhesion molecules, and migration within 3-D collagen lattices. *J. Leukoc. Biol.* **76,** 388–398 (2004).
44. Gloerich, M. *et al.* Spatial regulation of cyclic AMP-Epac1 signaling in cell adhesion by ERM proteins. *Mol. Cell Biol.* **30,** 5421–5431 (2010).
45. Cox, JJ. *et al.* An SCN9A channelopathy causes congenital inability to experience pain. *Nature* **444,** 894–898.

Acknowledgements

N.E. was supported by a Rubicon fellowship of the Netherlands Organisation for Scientific Research. J.M.T. was supported by José Castillejo fellowship JC2010-0196 granted by the Spanish Ministry of Science and Innovation. J.J.C. is supported by an MRC Research Career Development Fellowship. J.N.W. GL U.O. and G.S.H. were supported by WCU grant R31-2008-000-10103-0 at SNU. This work was also supported by an EU IMI Europain grant and BBSRC LOLA grant (J.N.W., J.E.L.) and the Wellcome Trust (J.N.W., M.S.M.). We are greatly indebted to Sam Gossage for excellent technical assistance.

Author contributions

N.E. and J.W. designed and supervised experiments. N.E. performed most of the *in vivo* and *in vitro* experiments. J.L. performed experiments to characterize hPiezo2. G.H and G.L. supervised by U.O., and J.T. and J.C. cloned hPiezo. L.B. performed the *in vivo* electrophysiology under the supervision of A.D. M.G. helped with the overexpression studies. M.M. performed surgery. Y.I. provided the Epac1 – / – mice. F.Z. provided the Epac constructs. N.E. and J.W. wrote manuscript with contributions of all authors. N.E., J.L. and L.B. contributed to data analysis and all authors contributed to the discussions.

Additional information

Supplementary Information accompanies this paper at http://www.nature.com/naturecommunications

Competing financial interests: The authors declare no competing financial interests.

Reprints and permission information is available online at http://npg.nature.com/reprintsandpermissions/

How to cite this article: Eijkelkamp N. *et al.* A role for Piezo2 in EPAC1-dependent mechanical allodynia. *Nat. Commun.* 4:1682 doi: 10.1038/ncomms2673 (2013).

Balancing GRK2 and EPAC1 levels prevents and relieves chronic pain

Huijing Wang,[1,2] Cobi J. Heijnen,[3] Cindy T.J. van Velthoven,[1] Hanneke L.D.M. Willemen,[1] Yoshihiro Ishikawa,[4] Xinna Zhang,[5] Anil K. Sood,[5] Anne Vroon,[1] Niels Eijkelkamp,[1] and Annemieke Kavelaars[3]

[1]Laboratory of Neuroimmunology and Developmental Origins of Disease, University Medical Center Utrecht, Utrecht, The Netherlands. [2]Department of Pharmacology, Shanghai Medical College, Fudan University, Shanghai, People's Republic of China. [3]Neuroimmunology of Cancer Related Symptoms (NICRS) Laboratory, Department of Symptom Research, University of Texas M.D. Anderson Cancer Center, Houston, Texas, USA. [4]Cardiovascular Research Institute, Yokohama City University Graduate School of Medicine, Yokohama, Japan. [5]Departments of Gynecologic Oncology and Cancer Biology, Center for RNA Interference and Non-Coding RNA, University of Texas M.D. Anderson Cancer Center, Houston, Texas, USA.

Chronic pain is a major clinical problem, yet the mechanisms underlying the transition from acute to chronic pain remain poorly understood. In mice, reduced expression of GPCR kinase 2 (GRK2) in nociceptors promotes cAMP signaling to the guanine nucleotide exchange factor EPAC1 and prolongs the PGE_2-induced increase in pain sensitivity (hyperalgesia). Here we hypothesized that reduction of GRK2 or increased EPAC1 in dorsal root ganglion (DRG) neurons would promote the transition to chronic pain. We used 2 mouse models of hyperalgesic priming in which the transition from acute to chronic PGE_2-induced hyperalgesia occurs. Hyperalgesic priming with carrageenan induced a sustained decrease in nociceptor GRK2, whereas priming with the PKCε agonist ΨεRACK increased DRG EPAC1. When either GRK2 was increased in vivo by viral-based gene transfer or EPAC1 was decreased in vivo, as was the case for mice heterozygous for *Epac1* or mice treated with *Epac1* antisense oligodeoxynucleotides, chronic PGE_2-induced hyperalgesia development was prevented in the 2 priming models. Using the CFA model of chronic inflammatory pain, we found that increasing GRK2 or decreasing EPAC1 inhibited chronic hyperalgesia. Our data suggest that therapies targeted at balancing nociceptor GRK2 and EPAC1 levels have promise for the prevention and treatment of chronic pain.

Introduction

According to a recent report by the NIH, chronic pain affects more than 100 million people in the United States (1). The same report concludes that increased understanding of the mechanisms contributing to the development of chronic pain is key to finding novel interventions by which to prevent it.

Inflammatory mediators induce pain by direct activation of nociceptive terminals, but also increase the sensitivity to painful stimuli, a phenomenon known as hyperalgesia (2–4). This inflammatory hyperalgesia is generated by peripheral sensitization of nociceptive neurons as well as by central sensitization at the level of the spinal cord (5–7). In most cases, inflammatory pain and hyperalgesia resolve after resolution of inflammation or after tissues heal. However, in a significant subset of patients, pain does not resolve, and chronic pain develops. For example, approximately 10%–15% of patients with herpes zoster–induced rash develop postherpetic pain, defined as pain lasting at least 3 months after healing of the rash (8). Chronic postsurgical pain is observed even more frequently, for example, in patients undergoing thoracotomy (50%), breast surgery (30%), or cholecystectomy (10%–20%) (9).

The mechanisms underlying the development of persistent pain are poorly understood, and this is a major limitation for identification of new and adequate treatments. At the level of signaling pathways in peripheral nociceptors, recent studies have shown that mammalian target of rapamycin– (mTOR-) and ERK-dependent pathways play a critical role in chronic pain (10–14). Models of hyperalgesic priming have been developed as a tool to study the transition to chronic pain (10, 15, 16). In these models, short-lasting hyperalgesia is induced by intraplantar injection of, for example, a low dose of carrageenan, the PKCε activator ΨεRACK (HDAPIGYD; pseudoreceptor octapeptide for activated PKCε), or the inflammatory cytokine IL-6 into the hind paw (10, 15, 16). After this transient period of hyperalgesia, changes occur in primary sensory neurons that lead to marked prolongation of the hyperalgesic response to a subsequent exposure to the inflammatory mediator PGE_2 (10, 15–17). Both mTOR- and ERK-dependent pathways play a critical role in nociceptive plasticity in hyperalgesic priming (10). In addition, in rats primed with carrageenan or ΨεRACK, prolonged PGE_2-induced hyperalgesia depends on activation of ERK and PKCε. In naive rats, the classic cAMP/PKA pathway is critical for the transient hyperalgesia in response to PGE_2 (17). cAMP-to-PKCε signaling is thought to be mediated via exchange protein directly activated by cAMP (EPAC; refs. 18, 19), and EPAC activation by intraplantar injection of the specific agonist 8-pCPT-2′-O-Me-cAMP (8-pCPT) induces hyperalgesia via a PKCε-dependent route (20).

We identified nociceptor GPCR kinase 2 (GRK2) as a novel regulator of the duration of inflammatory hyperalgesia (21–27). GRK2 restrains signaling by promoting desensitization of GPCRs (28) and/or by interacting with multiple components of intracellular signaling pathways (22, 29, 30).

Using sensory neuron–specific *Grk2*-heterozygous mice (SNS-*Grk2*$^{+/-}$ mice), which have a cell-specific approximately 50% decrease in nociceptor GRK2, we previously showed that mechanical hyperalgesia induced by PGE_2 and other cAMP-inducing agents was significantly prolonged in mice with low nociceptor GRK2 (22, 25). Inhibition of PKA did not affect PGE_2 hyperalgesia in SNS-*Grk2*$^{+/-}$

Conflict of interest: The authors have declared that no conflict of interest exists.
Citation for this article: *J Clin Invest.* 2013;123(12):5023–5034. doi:10.1172/JCI66241.

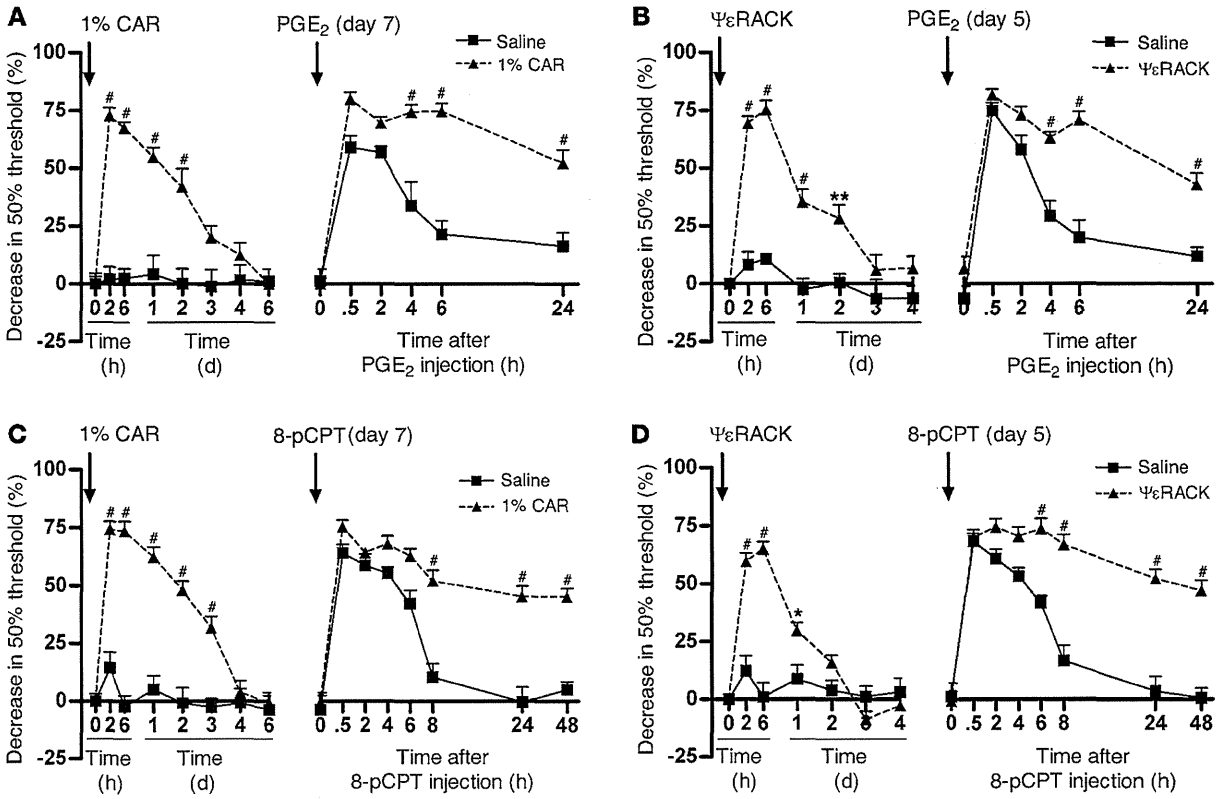

Figure 1

Hyperalgesic priming in mice. (**A** and **C**) 7 days after intraplantar carrageenan (CAR; 1%, 5 μl) or saline pretreatment or (**B** and **D**) 5 days after intraplantar ΨεRACK (1 μg/paw) or saline pretreatment, mice received an intraplantar injection of (**A** and **B**) PGE_2 (100 ng/paw) or (**C** and **D**) 8-pCPT (12.5 ng/paw). Changes in 50% paw withdrawal threshold were monitored over time. Data represent mean ± SEM. $n = 8$ per group. $^*P < 0.05$, $^{**}P < 0.01$, $^{\#}P < 0.001$.

mice, whereas inhibition of PKCε or ERK prevented the prolongation of PGE_2 hyperalgesia (22, 25). These findings indicate that the prolongation of PGE_2 hyperalgesia in GRK2-deficient mice involves activation of PKCε- and ERK-dependent signaling pathways (17, 22, 25). We also showed that GRK2 interacts with EPAC1 and inhibits EPAC signaling to its downstream target, RAP1 (22). Moreover, chronic inflammatory pain is associated with a decrease in GRK2 in nociceptors (25). In addition, Ferrari and coworkers showed that a transient decrease in GRK2 resulting from treating rats intrathecally with *Grk2* antisense oligodeoxynucleotides (asODNs) prolonged hyperalgesia, in this case via a PKCε-independent and PKA- and SRC tyrosine kinase–dependent mechanism (31).

Here we tested the hypothesis that protein levels of GRK2 and EPAC1 in nociceptors represent key factors regulating persistent hyperalgesia. Using 2 mouse models of hyperalgesic priming, prior nociceptive sensitization with carrageenan and with ΨεRACK, we showed that the induced transition to chronic PGE_2 hyperalgesia was mediated by decreased GRK2 and increased EPAC1, respectively. We also showed that the prolongation of PGE_2 hyperalgesia in primed mice was inhibited by either upregulation of GRK2 or downregulation of EPAC1 after development of the primed state. These effects occurred regardless of whether GRK2 was decreased or EPAC1 was increased. Changing the balance between GRK2 and EPAC1 may have more general relevance for hyperalgesia, as we also showed using the CFA model of chronic inflammatory pain, in which increasing GRK2 or downregulating EPAC1 inhibited persistent mechanical hyperalgesia.

Results

Hyperalgesic priming. Hyperalgesic priming was induced in mice with an intraplantar injection of carrageenan or ΨεRACK. At 7 days after carrageenan and 5 days after ΨεRACK injection, primed mice received an intraplantar injection of PGE_2 or the EPAC activator 8-pCPT.

In carrageenan-primed mice, PGE_2-induced mechanical hyperalgesia lasted more than 24 hours, whereas in saline-treated mice, PGE_2 hyperalgesia resolved within 6 hours (Figure 1A). In ΨεRACK-primed mice, PGE_2 hyperalgesia was also prolonged to more than 24 hours (Figure 1B). Moreover, hyperalgesia induced by 8-pCPT exceeded 48 hours in carrageenan- and ΨεRACK-primed mice, compared with less than 8 hours in control mice (Figure 1, C and D).

Carrageenan priming also prolonged hyperalgesia induced by the cAMP-inducing mediator epinephrine from 4 days in control mice to almost 2 weeks in primed mice (Supplemental Figure 1A; supplemental material available online with this article; doi:10.1172/JCI66241DS1). Interestingly, carrageenan priming did not affect hyperalgesia induced by IL-1β (Supplemental Figure 1B), a proinflammatory mediator that does not induce cAMP signaling, but promotes hyperalgesia via a p38-mediated pathway.

GRK2 levels in primary sensory neurons of primed mice. We next determined whether hyperalgesic priming by carrageenan

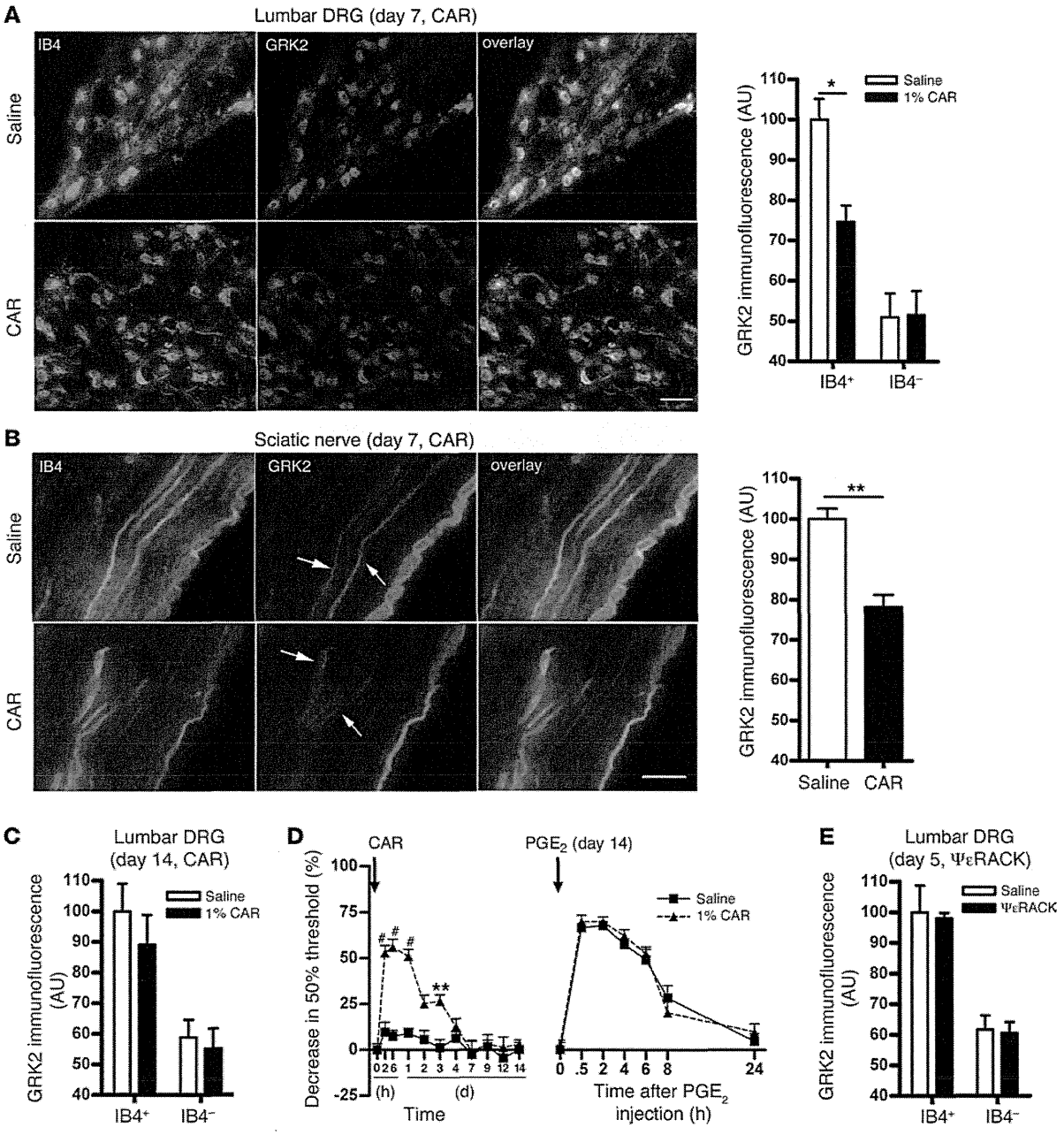

Figure 2

Carrageenan- and ΨεRACK-induced changes in sensory neuron GRK2 protein expression. (**A** and **B**) Mice received an intraplantar injection of 1% carrageenan or saline, and 7 days later, GRK2 protein levels in IB4$^+$ and IB4$^-$ neurons from lumbar DRG, thoracic DRG, and sciatic nerve fibers were quantified by immunofluorescence analysis. Shown are representative images of IB4 (green) and GRK2 (red) double staining of (**A**) lumbar DRG and (**B**) sciatic nerves, and mean GRK2 immunofluorescence intensity in (**A**) lumbar or thoracic DRG and (**B**) sciatic nerve fibers. Scale bars: 50 μm. (**C**) Mean GRK2 immunofluorescence intensity in lumbar DRG at 14 days after intraplantar carrageenan or saline. (**D**) 14 days after carrageenan or saline pretreatment, mice received an intraplantar injection of PGE_2 (100 ng/paw). Changes in 50% paw withdrawal threshold were monitored over time. (**E**) Mean GRK2 immunofluorescence intensity in lumbar DRG at 5 days after intraplantar ΨεRACK or saline. Data represent mean ± SEM (n = 4 per group), based on approximately 300 neurons from lumbar DRG per mouse. $^*P < 0.05$, $^{**}P < 0.01$, $^{\#}P < 0.001$.

decreases neuronal GRK2 protein levels in dorsal root ganglion (DRG) and sciatic nerve. Because the isolectin B4–positive (IB4$^+$) subpopulation of DRG neurons is known to be involved in hyperalgesic priming (32, 33), we used IB4 as a marker to identify this specific subgroup of sensory neurons.

At 3 and 7 days after intraplantar carrageenan injection into the hind paws, the level of GRK2 in small-diameter IB4$^+$ neurons was reduced by approximately 25% in lumbar DRG (Figure 2A and Supplemental Figure 2). There was no change in GRK2 protein levels in small-diameter IB4$^-$ neurons in lumbar DRG after

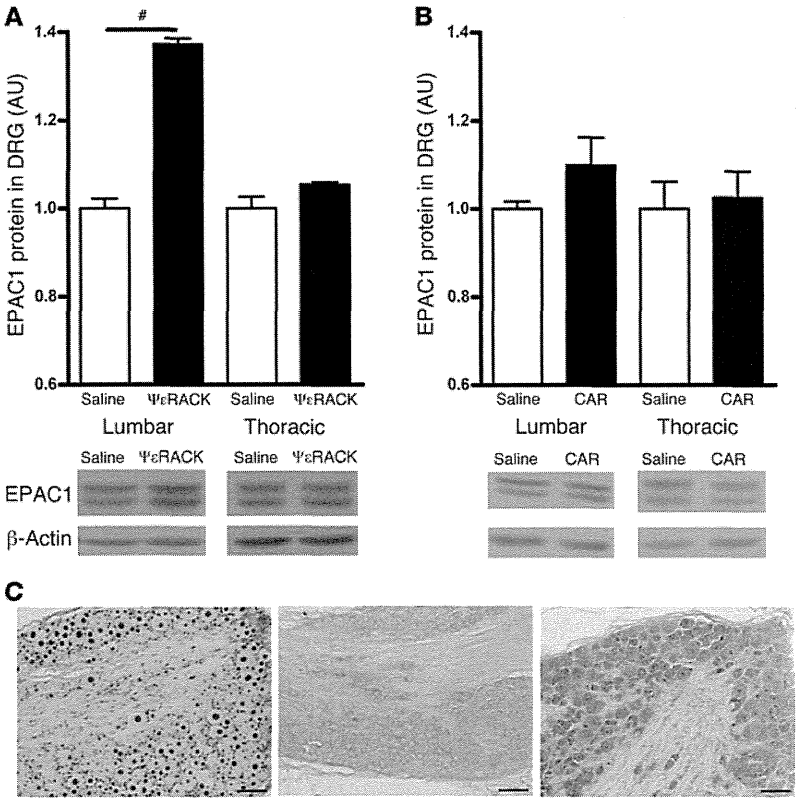

Figure 3
EPAC1 level in DRG after carrageenan- and ΨεRACK-induced priming. (**A** and **B**) EPAC1 protein level in DRG, determined by Western blot analysis of DRG tissue homogenates, at (**A**) 5 days after ΨεRACK priming and (**B**) 7 days after carrageenan priming. Data represent mean ± SEM (n = 4 per group). $^{\#}P < 0.001$. (**C**) Cellular distribution of *Epac1* mRNA expression was analyzed by in situ hybridization analysis of lumbar DRG from untreated mice. Representative example from 1 mouse of 3 with similar results. Left: Nuclear staining of positive control (U6 small nuclear RNA probe). Middle: Negative control probe. Right: *Epac1* probe. Scale bars: 20 μm.

carrageenan priming (Figure 2A and Supplemental Figure 2). In addition, GRK2 levels did not change in thoracic DRG neurons at any time point (Supplemental Figure 3). Western blot analysis of DRG homogenates did not detect changes in GRK2 protein at day 7 after carrageenan priming (Supplemental Figure 4). This is likely due to reduced GRK2 only in IB4$^+$ sensory neurons in response to intraplantar carrageenan.

The carrageenan-induced GRK2 decrease in the soma of IB4$^+$ sensory neurons was also reflected in a decrease in axonal GRK2; at 7 days after carrageenan injection, the level of GRK2 in IB4$^+$ fibers was reduced by approximately 20% in the carrageenan- versus the saline-pretreated group (Figure 2B).

At day 14 after intraplantar carrageenan injection, GRK2 levels in small-diameter IB4$^+$ sensory neurons had returned to baseline levels (Figure 2C). The primed state had also resolved at 14 days after carrageenan injection; the course of PGE_2 hyperalgesia did not differ between the saline- and carrageenan-pretreated groups at this time point (Figure 2D). These findings show that resolution of the primed state is associated with normalization of GRK2 protein levels.

Notably, when we evaluated GRK2 levels in lumbar DRG at 5 days after ΨεRACK priming, we did not observe any change in GRK2 level. The levels of GRK2 were similar in small-diameter IB4$^+$ lumbar sensory neurons from ΨεRACK-primed and saline-treated mice (Figure 2E). Furthermore, no changes in GRK2 levels were observed in IB4$^-$ lumbar DRG neurons or in thoracic DRG neurons after ΨεRACK priming (Supplemental Figure 3).

EPAC1 level in DRG after carrageenan and ΨεRACK priming. After both carrageenan and ΨεRACK priming, hyperalgesia induced by 8-pCPT was significantly prolonged. These findings indicate that in both cases, the primed state is associated with a prolonged hyperalgesic response to EPAC activation. We hypothesized that either a decrease in GRK2 or an increase in EPAC1 would be sufficient to facilitate EPAC1-mediated signaling leading to prolonged PGE_2 hyperalgesia. To test this hypothesis, we measured the level of EPAC1 in DRG in these 2 priming conditions. The antibodies available for EPAC1 did not allow reliable staining for this protein in sensory neurons. Therefore, we analyzed EPAC1 levels by Western blotting. EPAC1 levels in lumbar DRG of ΨεRACK-primed mice were increased by approximately 35% compared with levels in saline-treated mice, whereas carrageenan priming did not induce a detectable change in EPAC1 (Figure 3, A and B). To determine which cells in the DRG express EPAC1, we used an in situ hybridization approach. Virtually all neurons in the DRG stained positively for *Epac1* mRNA (Figure 3C).

Effect of GRK2 gene transfer on treatment of hyperalgesic priming. To determine whether the observed changes in GRK2 and EPAC1 levels in the DRG represent potential targets for the prevention of chronic pain, we first examined the effect of increasing GRK2 in DRG neurons in vivo after hyperalgesic priming with carrageenan and ΨεRACK. We used a herpes simplex virus (HSV; ref. 34) vector encoding bovine *GRK2* and *GFP* as a reporter protein (referred to herein as HSV-*GRK2*) or a control HSV vector containing *GFP* only (HSV-*GFP*). In carrageenan-primed mice, treatment with 2.5 μl of 1.4×10^7 pfu/ml HSV-*GRK2* at days 3 and 5 significantly shortened PGE_2 hyperalgesia compared with mice treated with HSV-*GFP* (Figure 4A). In ΨεRACK-primed mice, HSV-*GRK2* also shortened PGE_2 hyperalgesia compared with mice treated with the same dose of HSV-*GFP* (Figure 4B). This effect of *GRK2* overexpression occurred even though ΨεRACK priming did not induce a detectable decrease in GRK2 protein in DRG neurons (Figure 2E).

PGE_2 hyperalgesia lasted about 8 hours in both HSV-*GRK2*– and HSV-*GFP*–treated mice that had not been exposed to carrageenan or ΨεRACK (Figure 4C), which indicates that in naive mice, *GRK2* overexpression in sensory neurons does not affect the pain response.

Inoculation with HSV induced a transient and small increase in mechanical sensitivity that resolved within 1–2 days and was independent of the presence of *GRK2* (Figure 4, A–C). Therefore, it is unlikely that this acute response to the virus contributed to the observed inhibition of the primed phenotype.

To confirm successful *GRK2* gene transfer, we analyzed expression of the *GFP* reporter in lumbar DRG, sciatic nerve, and skin of the injected paw 3 days after the last HSV injection. GFP

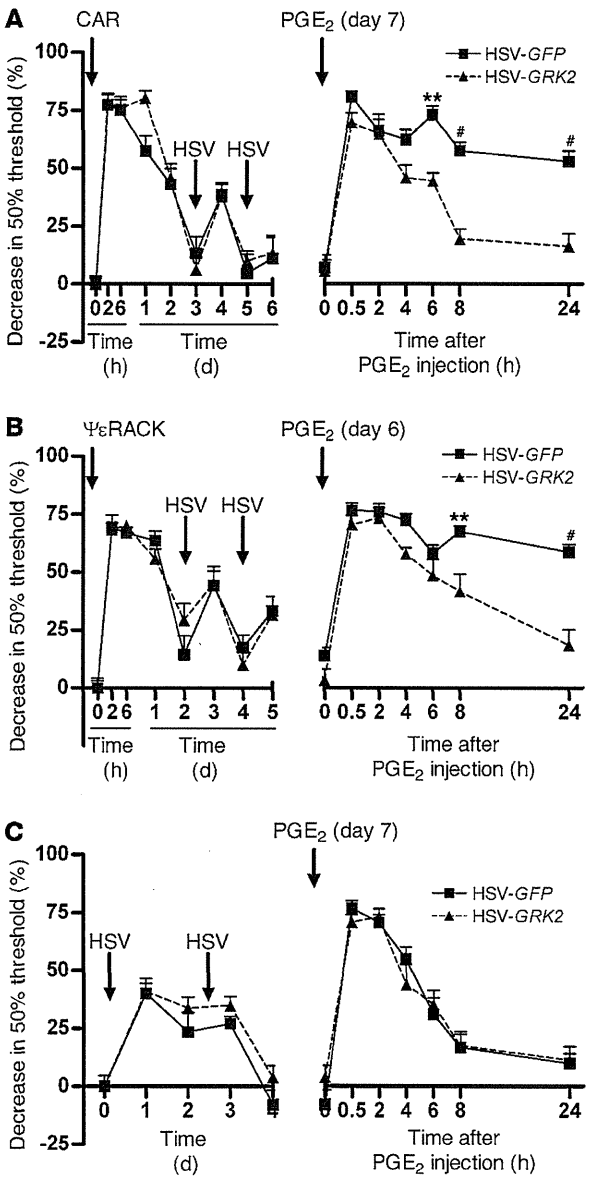

Figure 4
Effect of HSV-mediated GRK2 overexpression on carrageenan- and ΨεRACK-induced hyperalgesic priming. (**A**) Carrageenan-primed, (**B**) ΨεRACK-primed, or (**C**) naive control mice were inoculated intraplantarly with 2 injections of HSV-*GRK2* or HSV-*GFP* (1.4×10^7 pfu/ml, 2.5 μl/paw) followed by PGE_2 (100 ng/paw). Changes in 50% paw withdrawal threshold were monitored over time. Data represent mean ± SEM ($n = 8$ per group). $^{**}P < 0.01$, $^{\#}P < 0.001$.

expression was clearly visible in both IB4$^+$ and IB4$^-$ small-diameter DRG neurons and in both IB4$^+$ and IB4$^-$ fibers in the sciatic nerve (Figure 5, A–F). GFP was also detected in peripherin$^+$ nerves in the skin (Figure 5, G–I).

Next, we determined whether GRK2 kinase activity is required to prevent transition to chronic pain after priming, using an HSV construct expressing *GRK2*^{K220R}, the kinase-dead mutant of *GRK2* (35). *GRK2*^{K220R} did not reverse the primed state (Figure 6). The course of PGE_2 hyperalgesia in primed mice treated with HSV-*GRK2*^{K220R} was similar to that of primed mice receiving control HSV-*GFP* inoculation.

Collectively, our data indicate that, independently of whether priming decreased GRK2 or increased EPAC1 expression, HSV-mediated *GRK2* overexpression was sufficient to reverse the primed state, thereby preventing the development of persistent hyperalgesia.

Hyperalgesic priming in Epac1$^{+/-}$ *mice.* To further test our hypothesis that the GRK2/EPAC1 system regulates the transition to chronic hyperalgesia in primed mice, we used mice with heterozygous knockout of *Epac1* (*Epac1*$^{+/-}$ mice; ref. 36). These mice had an approximately 50% reduction in EPAC1 protein in the DRG (Figure 7A). In response to carrageenan and ΨεRACK priming, *Epac1*$^{+/-}$ mice did not show the prolongation of PGE_2 hyperalgesia observed in WT mice (Figure 7, B and C). The course of PGE_2 hyperalgesia did not differ between *Epac1*$^{+/-}$ and WT mice that were not primed (Figure 7D).

Effect of intrathecal Epac1 asODNs on hyperalgesic priming. The results we obtained in *Epac1*$^{+/-}$ mice suggested that hyperalgesic priming can be prevented by lowering EPAC1 levels. We next tested whether the primed state can also be treated by temporarily downregulating EPAC1 protein levels in sensory neurons using intrathecal injection of *Epac1* asODNs. *Epac1* asODN treatment significantly reduced the duration of PGE_2 hyperalgesia in mice primed with carrageenan or ΨεRACK (Figure 8, A and C). In lumbar DRG, protein levels of EPAC1 in carrageenan- and ΨεRACK-primed mice decreased significantly after intrathecal *Epac1* asODN injection (Figure 8, B and D).

The *Epac1* asODN–mediated decrease in EPAC1 protein levels did not change the baseline mechanical pain threshold or the duration and severity of acute PGE_2 hyperalgesia in naive mice (Figure 8, E and F). Intrathecal administration of *Epac1* asODNs did not affect the protein levels of EPAC2 (Supplemental Figure 5).

Effect of HSV-GRK2 or intrathecal Epac1 asODN in a model of chronic inflammatory pain. To determine the broader relevance of the GRK2/EPAC1 system for chronic pain, we used the CFA model of chronic inflammatory pain. HSV-*GRK2* treatment significantly attenuated the chronic mechanical hyperalgesia that developed in response to CFA (Figure 9A). Intrathecal administration of *Epac1* asODNs also reduced the chronic CFA-induced mechanical hyperalgesia (Figure 9B). In CFA-treated mice, GRK2 levels in IB4$^+$ DRG neurons were decreased at day 5 after CFA injection (Figure 9C). We did not detect changes in GRK2 protein by Western blot analysis (Supplemental Figure 6). Consistent with earlier studies (37), DRG EPAC1 levels were increased in CFA-treated mice (Figure 9D).

Discussion

Although it is widely accepted that acute and chronic pain are different entities that depend on specific neurobiological pathways, knowledge about the underlying mechanisms remains limited. Here, we uncovered 2 key regulators of the development and maintenance of persistent pain in response to repeat or chronic inflammation: the kinase GRK2, and the cAMP sensor EPAC1. Specifically, using carrageenan and ΨεRACK priming as mouse models of the transition to persistent hyperalgesia, we showed that the prolongation of the hyperalgesic response in primed mice is associated with a sustained decrease in GRK2 level or increase in EPAC1 level in DRG (Figure 10). The functional importance of this observation is attested by our findings that increasing nociceptor GRK2 or decreasing EPAC1 prevented per-

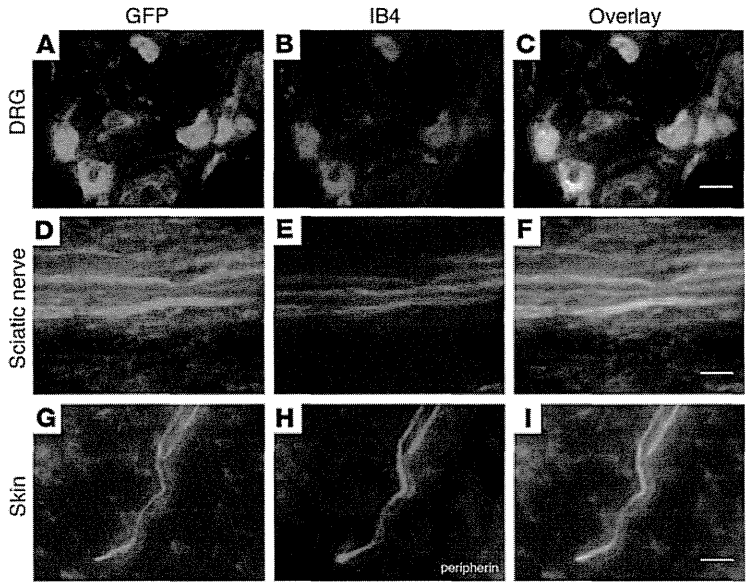

Figure 5
HSV-mediated overexpression of *GRK2* and *GFP*. Expression of GFP (**A**, **D**, and **G**), an indicator of successful transgene expression, was observed in IB4$^+$ lumbar DRG neurons (**B**), IB4$^+$ sciatic nerve fibers (**E**), and peripherin$^+$ nerve endings (**H**) in the skin at 2 days after the last inoculation with HSV-*GRK2* in primed mice. (**C**, **F**, and **I**) Merged images showing overlay. Scale bars: 20 μm.

sistent hyperalgesia in primed mice. Notably, increasing GRK2 expression prevented the prolongation of PGE_2 hyperalgesia in primed mice, regardless of whether GRK2 was decreased (after carrageenan priming) or EPAC1 was increased (after ΨεRACK priming). Similarly, downregulating EPAC1 inhibited the primed phenotype when GRK2 was decreased without a change in EPAC1 (in the carrageenan model), as well as when GRK2 was unchanged and EPAC1 was increased (in the ΨεRACK model). On the basis of these novel findings, we propose that an imbalance between the protein levels of GRK2 and EPAC1 is sufficient to cause the prolongation of hyperalgesia in primed mice. We also propose that reestablishing the GRK2/EPAC1 balance can be considered as a novel avenue for the prevention of persistent pain.

Importantly, the role of GRK2 and EPAC1 is not restricted to persistent hyperalgesia in priming models. In the well-established model of CFA-induced chronic inflammatory pain, DRG GRK2 was increased and EPAC1 decreased. Moreover, increasing GRK2 or decreasing EPAC1 during ongoing inflammatory pain inhibited chronic CFA-induced hyperalgesia. This is important because it indicates that targeting GRK2/EPAC1 may both prevent chronic pain and combat existing chronic pain, such as that experienced by patients with painful inflammatory diseases like arthritis.

We confirmed earlier findings that DRG EPAC1 levels are increased in the CFA model of chronic inflammatory pain (37). In addition, we showed that the CFA model was associated with reduced GRK2 in IB4$^+$ nociceptors. Interestingly, the mechanical hyperalgesia that develops in the CFA model was inhibited by increasing nociceptor GRK2 or by decreasing EPAC1 levels. DRG EPAC1 levels are also increased in the L5 spinal nerve transection model of chronic neuropathic pain in mice (38). In addition, nerve damage–induced mechanical hyperalgesia was significantly reduced in *Epac1*$^{+/-}$ and *Epac1*$^{-/-}$ mice (38). In vitro, EPAC1 signaling enhances Piezo2-mediated mechanotransduction in sensory neurons (38). Our findings demonstrated that EPAC1 is also a key to promoting mechanical hyperalgesia in primed mice as well as in a classic model of chronic inflammatory pain. Moreover, our findings indicate that decreased nociceptor GRK2 promotes persistent hyperalgesia in a priming model and contributes to chronic inflammatory pain. It remains to be determined whether HSV-*GRK2*–mediated overexpression of GRK2 also attenuates chronic neuropathic pain.

In naive animals, cAMP-inducing agents such as PGE_2 and epinephrine induce hyperalgesia via the classic cAMP target PKA (17, 22, 25). However, in primed rats or in mice with genetically low

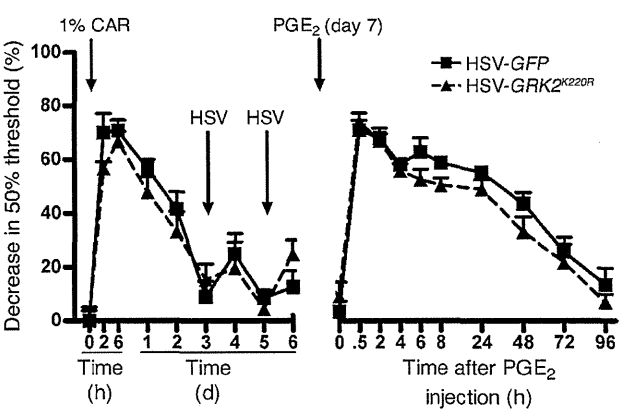

Figure 6
Effect of overexpression of the *GRK2* kinase-dead mutant, *GRK2*^{K220R}, on carrageenan-induced hyperalgesic priming. Carrageenan-primed mice were inoculated intraplantarly with 2 injections of HSV-*GRK2*^{K220R} or HSV-*GFP* followed by PGE_2 (100 ng/paw). Changes in 50% paw withdrawal threshold were monitored over time. Data represent mean ± SEM (n = 8 per group).

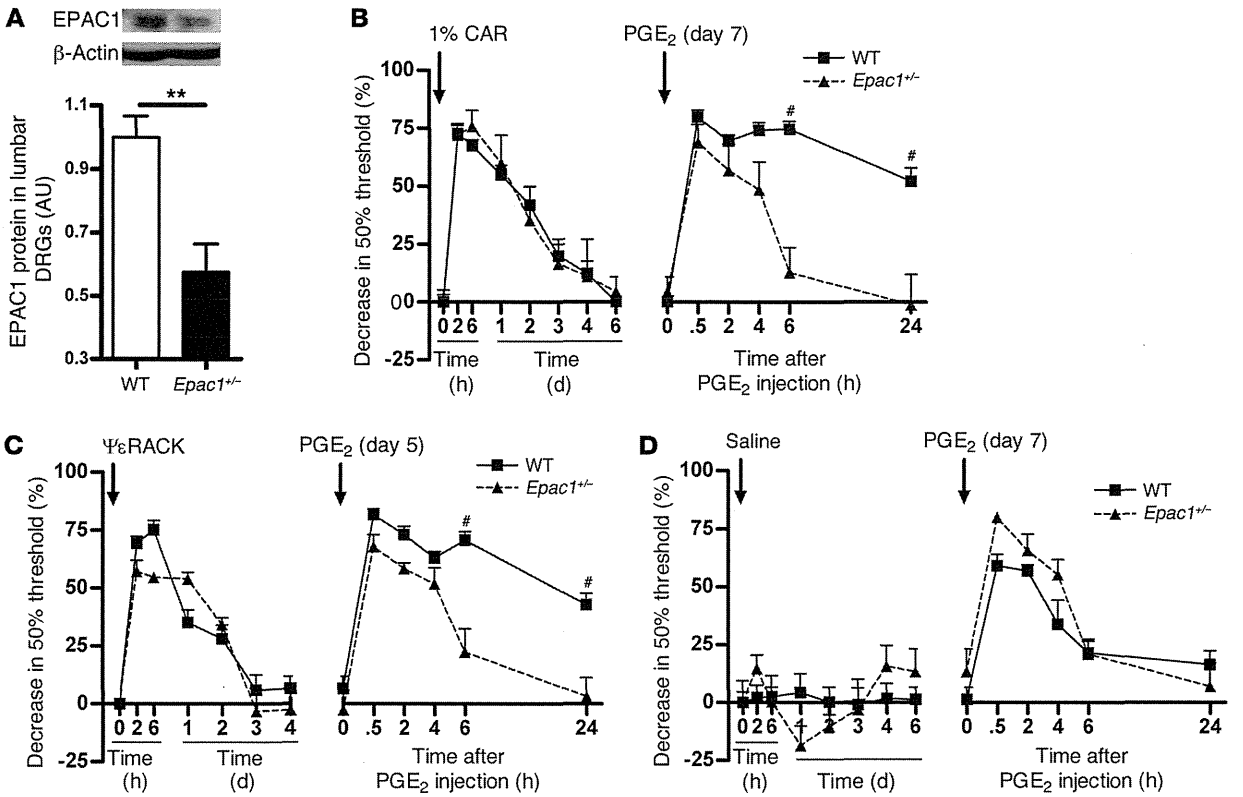

Figure 7

Hyperalgesic priming in *Epac1*$^{+/-}$ mice. (**A**) EPAC1 protein level, determined by Western blot analysis of DRG tissue homogenates from WT and *Epac1*$^{+/-}$ mice ($n = 4$ per group). (**B**) 7 days after carrageenan pretreatment ($n = 4$ per group), (**C**) 5 days after intraplantar ΨεRACK pretreatment (1 μg/paw in 5 μl saline; $n = 6$ per group), or (**D**) 7 days after saline pretreatment ($n = 4$ per group), mice received an intraplantar injection of PGE_2 (100 ng/paw in 2.5 μl saline). Changes in 50% paw withdrawal threshold were monitored over time. Data represent mean ± SEM. $^{**}P < 0.01$, $^{\#}P < 0.001$.

levels of nociceptor GRK2, inhibition of PKA does not inhibit hyperalgesia induced by these agents. In primed rats or nociceptor GRK2–deficient mice, inhibition of PKCε or ERK prevents prolongation of 8-Br-cAMP, PGE_2, or epinephrine hyperalgesia. These findings indicate that priming and *Grk2* deficiency both promote ERK- and PKCε-mediated hyperalgesic signaling in response to cAMP-inducing agents (17, 22, 25). Levine and colleagues were the first to show that activation of the alternative cAMP sensor EPAC induces hyperalgesia via a PKCε-mediated pathway (20). Hyperalgesia induced by 8-pCPT is also prolonged in conditions of SNS-*Grk2* deficiency (22). Moreover, in vitro, low GRK2 promotes 8-pCPT signaling to the EPAC target RAP1 and to ERK (22). On the basis of these earlier in vitro findings and our present in vivo findings, we hypothesize that the shift in the balance between GRK2 and EPAC1 levels in the DRG in primed mice and in mice with chronic inflammatory pain may promote EPAC1 signaling and persistent mechanical hyperalgesia. Consistently, hyperalgesia induced by 8-pCPT was prolonged after priming with carrageenan as well as ΨεRACK. Treatment of primed mice with HSV-*GRK2*^{K220R} did not reverse the primed state, which indicates that GRK2 kinase activity is required for inhibiting pain signaling. Future studies should investigate whether GRK2 directly phosphorylates EPAC1 to inhibit EPAC1 activation and control the pain response.

Earlier studies have shown that activation of the mTOR pathway and protein translation in the periphery are required for development of IL-6– and carrageenan-induced priming of the subsequent response to PGE_2 (10, 11, 17, 39). Axonal protein synthesis under the control of mTOR and ERK activation contribute to chronic pain in multiple other models as well (12–14). ERK activation also contributes to the prolonged PGE_2 hyperalgesia in *Grk2*-deficient mice, and ERK activation by 8-pCPT is increased in *Grk2*-deficient cells (22). Notably, stimulation of prostate cancer cells with 8-pCPT activates the mTOR pathway (40, 41). Thus, it is conceivable that increased EPAC signaling promotes persistent pain via downstream activation of ERK and mTOR signaling pathways, leading to peripheral protein translation.

GRK2 protein is reduced in peripheral blood lymphocytes from humans with rheumatoid arthritis or multiple sclerosis (42, 43) and in splenocytes from rats with adjuvant arthritis or EAE (44, 45). In all these examples, the reduction in GRK2 was not associated with a change in *Grk2* mRNA, which indicates that regulation takes place at the posttranslational level. The inflammation in rats with adjuvant arthritis spontaneously resolves approximately 30 days after induction. However, GRK2 levels in splenocytes were still reduced by 50% 2 weeks after resolution of inflammation (44). Similarly, we showed here that GRK2 levels in DRG neurons remained decreased even after resolution of the inflammation-

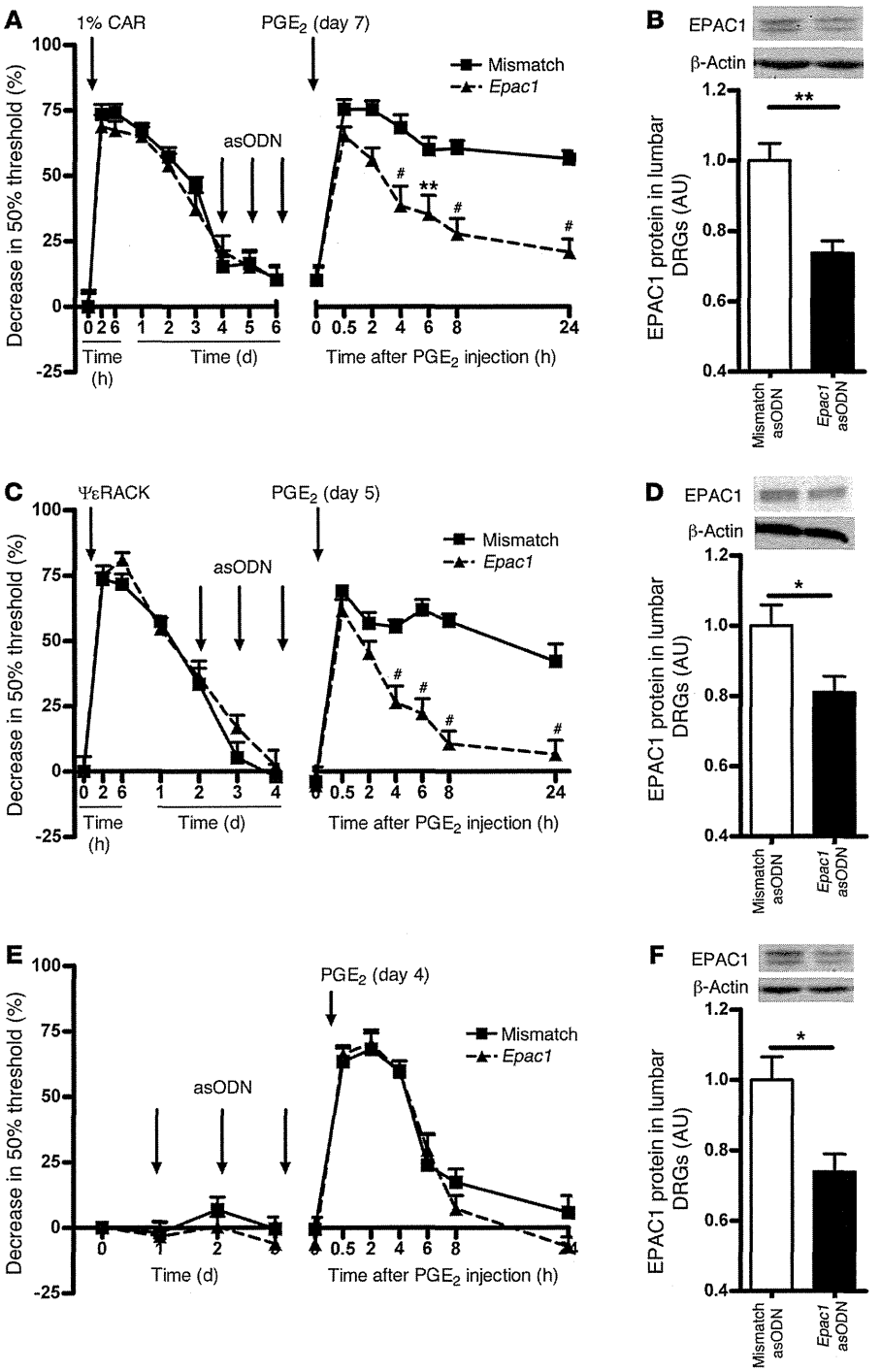

Figure 8
Effect of intrathecal *Epac1* asODNs on carrageenan- and ΨεRACK-induced hyperalgesic priming. 3 days before intraplantar PGE_2 injection (100 ng/paw, in 2.5 μl saline), mice primed with (**A** and **B**) carrageenan or (**C** and **D**) ΨεRACK or (**E** and **F**) naive mice received 3 daily intrathecal injections of *Epac1* or mismatch control asODNs. (**A**, **C**, and **E**) Changes in 50% paw withdrawal threshold were monitored over time ($n = 8$ per group). (**B**, **D**, and **F**) EPAC1 levels were determined by Western blot 2 days after the last asODN treatment ($n = 4$ per group). Data represent mean ± SEM. $^*P < 0.05$, $^{**}P < 0.01$, $^{\#}P < 0.001$.

induced hyperalgesia. Very little is known about regulation of the cellular level of EPAC1, and it remains to be determined via which mechanism the amount of GRK2 protein is kept at a lower level in IB4$^+$ nociceptors or the DRG EPAC1 content is maintained at a higher level during the primed state.

Both in the carrageenan model of hyperalgesic priming and in the CFA model of chronic inflammatory pain, the reduction in GRK2 expression was restricted to small-diameter IB4$^+$ sensory neurons. It is well known that specific sets of sensory neurons are involved in different pain modalities and, more importantly, different types of chronic pain (46–49). The IB4$^+$ subset of DRG neurons specifically responds to inflammatory stimuli injected intraplantarly (46–49). Depletion of IB4$^+$ neurons completely ablates the primed phenotype, which indicates that priming induces changes with functional consequences specifically for IB4$^+$ neurons (32, 33). Moreover, selective changes occur in specific sets of neurons during inflammatory pain, including specific changes limited to IB4$^+$ neurons (33, 50, 51). It remains to be determined,

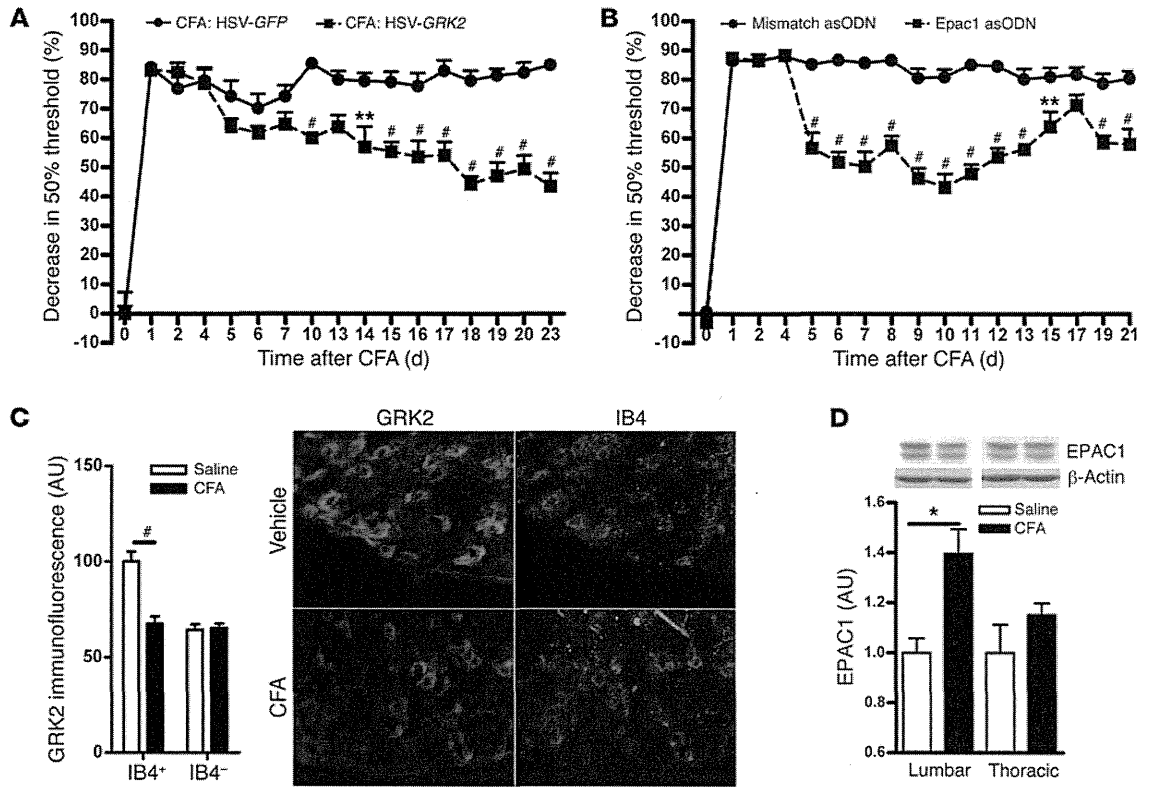

Figure 9

Effect of intraplantar HSV-*GRK2* or intrathecal *Epac1* asODNs on mechanical hyperalgesia in CFA-induced chronic inflammatory pain. (**A** and **B**) Mice were treated (**A**) intraplantarly with HSV-*GRK2* or HSV-*GFP* on days 4, 6, 13, and 16 after intraplantar CFA (n = 6 per group) or (**B**) intrathecally with *Epac1* or mismatch asODNs on days 4, 5, 6, 8, and 10 after intraplantar CFA (n = 8 per group). Changes in 50% paw withdrawal threshold were monitored over time. (**C**) Lumbar DRG were collected on day 5 after intraplantar CFA or saline, and GRK2 protein levels in DRG neurons were analyzed as described in Figure 1. Scale bar: 50 μm. (**D**) EPAC1 protein levels in lumbar DRG were quantified by Western blotting at day 5 after intraplantar saline or CFA (n = 4 per group). Data represent mean ± SEM. $^*P < 0.05$, $^{**}P < 0.01$, $^{\#}P < 0.001$.

however, which mechanisms govern the decrease in GRK2 specifically in IB4$^+$ small-diameter DRG neurons.

GRK2 was decreased in IB4$^+$ DRG neurons in the carrageenan model of hyperalgesic priming as well as in the CFA model of chronic inflammatory pain that depends on Nav1.8$^+$ nociceptors (52). After administration of HSV-*GRK2*, the GFP reporter protein was detected predominantly in IB4$^+$ small-diameter neurons and in IB4$^+$ nerve fibers in the sciatic nerve. This distribution of transgene expression after HSV-mediated gene transfer is consistent with earlier reports (53) and highlights HSV-mediated gene transfer as a specific tool by which to target small-diameter sensory neurons important in inflammatory pain processing. Nociceptor-specific targeting of GRK2 might prevent adverse effects in large-diameter neurons, likely leaving touch sensations unaffected (53). Indeed, mechanical sensitivity in naive mice, as determined using von Frey hairs, was unaffected by HSV-*GRK2*. Similarly, *Grk2*-deficient mice exhibit normal heat sensitivity under baseline conditions (21). Whether acute nociception of noxious stimuli such as mechanical pressure or heat is affected by changing EPAC1 levels remains to be determined.

HSV-*GRK2* treatment shortened PGE_2 hyperalgesia in primed mice and attenuated CFA-induced chronic hyperalgesia. These findings are consistent with our hypothesis that reduced GRK2 in IB4$^+$ nociceptors is a key factor that contributes to priming and to chronic inflammatory pain. Unfortunately, the available EPAC1 antibodies did not allow reliable quantification of EPAC1 expression in DRG neurons by immunohistochemistry, and therefore we do not know in which DRG neurons EPAC1 levels were increased after priming. However, in situ hybridization analysis demonstrated that *Epac1* mRNA was expressed in all cells in the DRG, including small-diameter neurons. We also showed that reducing DRG EPAC1 expression reversed the primed phenotype; this was the case even when DRG EPAC1 levels were not affected as GRK2 levels increased in small-diameter IB4$^+$ neurons. Notably, expression of GRK2 using the HSV-*GRK2* amplicon also inhibited the primed phenotype when GRK2 levels were not affected as EPAC1 levels were increased, for example, after ΨεRACK priming. Taken together, these findings support the hypothesis that a GRK2/EPAC1-dependent pathway in small-diameter nociceptors contributes to the primed phenotype. However, we cannot presently exclude that other, or additional, effects of changing GRK2 and EPAC1 levels in these and other cells ultimately are responsible for the observed inhibition of the primed phenotype when increasing GRK2 or decreasing EPAC1.

GRK2 and EPAC1 are widely expressed in both human and rodent tissues, including brain, heart, and thyroid gland, and

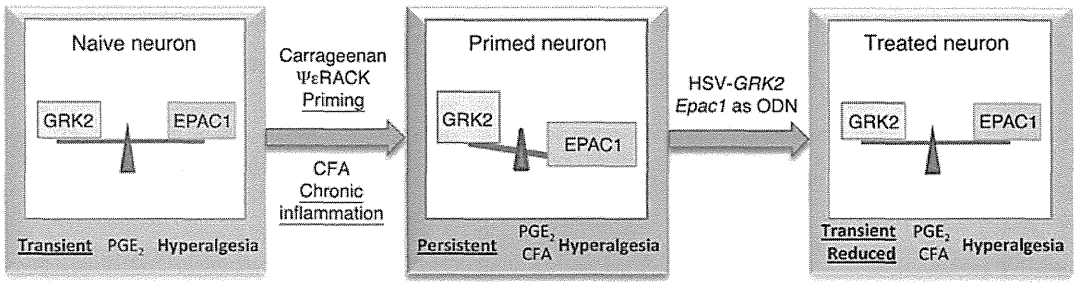

Figure 10
Schematic representation of our working model. Decreased GRK2 in peripheral sensory neurons and/or increased EPAC1 promotes the development of persistent hyperalgesia. Treatment with intraplantar HSV-*GRK2* or intrathecal *Epac1* asODNs normalizes the GRK2/EPAC1 balance, leading to inhibition of persistent hyperalgesia.

are likely to regulate a wide array of physiological processes (18, 19, 54–58). Therefore, changes in the protein levels of GRK2 and EPAC1 in other tissues may have important consequences for cAMP signaling and (patho)physiology. This potentially widespread importance of GRK2/EPAC1 makes it unlikely that systemic treatments aimed at increasing GRK2 or decreasing EPAC1 will be of therapeutic benefit. The approach we used here, in which we locally administered HSV amplicons to overexpress *GRK2* specifically in the area in which the increased pain response occurs, may be much more relevant. Another benefit of targeting the GRK2/EPAC system in sensory neurons is that by directly targeting intracellular signaling pathways involved in the transition to chronic pain, only the "pathological" transition to chronic pain is targeted, while evolutionary beneficial acute pain is not affected. Indeed, our data showed that increasing GRK2 in naive mice did not affect acute mechanical PGE_2 hyperalgesia. In addition, acute carrageenan and ΨεRACK priming–induced hyperalgesia was unaffected in *Epac1*$^{+/-}$ mice.

The important question arises as to whether the priming phenomenon occurs in humans. A recent experimental study in humans showed that pre-exposure to a mild inflammatory stimulus (low-dose endotoxin) increased the hyperalgesic response to subsequent intradermal injection of capsaicin (59). Clinically, there is evidence that repeat surgery for recurring inguinal hernia increases the risk of chronic postoperative pain (9, 60, 61). In addition, gastrointestinal infection is a risk factor for irritable bowel disorder, a condition in which, for example, ingestion of food can induce a pain response (62). These observations indicate that in humans, previous exposure to tissue damage and/or inflammation may also sensitize (prime) the pain response to subsequent challenge, reminiscent of hyperalgesic priming. Increasing EPAC1 or decreasing GRK2 prevented the development of persistent hyperalgesia in mice primed by transient local inflammation. Therefore, we propose that targeting GRK2/EPAC1 prior to repeat surgery or in patients with irritable bowel disorder may help prevent or treat persistent pain in these situations that resemble hyperalgesic priming. Perhaps more importantly, we also showed that targeting GRK2/EPAC1 inhibited CFA-induced hyperalgesia, a model of persistent inflammatory pain. On the basis of these results, we propose that patients with chronic pain associated with chronic inflammation (e.g., arthritic pain) could benefit from therapies targeting GRK2/EPAC1. This may be especially relevant for patients that continue to experience pain after apparently successful reduction of joint inflammation in response to treatment (63, 64). Preclinical studies should be performed to further examine these possibilities.

Local application of HSV is regarded as an ideal platform for novel therapies of chronic pain because HSV has a natural ability to infect the sensory nerve via peripheral inoculation. With a single inoculation, the virus may provide long-term therapy in restricted appropriate regions of the body (65, 66). Recently, results from a phase I clinical trial using a similar replication-deficient HSV amplicon to overexpress preproenkephalin reported no adverse effects in patients (67). Notably, a recent study in rats indicates that HSV amplicons can also be used for the targeted delivery of asODNs (68), and thus would provide a tool to locally reduce EPAC1 expression as well. These and our present findings clearly indicate that it may ultimately be feasible to use a similar approach in humans to deliver GRK2 by local administration of HSV-*GRK2* or *EPAC1* antisense DNA in humans to prevent and treat chronic pain.

Methods

Animals. Female C57BL/6 mice as well as *Epac1*$^{+/-}$ (36) and littermate WT mice aged 12–14 weeks were used. All experiments were performed in a blinded setup.

Mechanical hyperalgesia. Before experiments, mice were exposed to the equipment without any nociceptive stimulation for 1–2 h/d for 2 days. On day 3, mice were placed in the test environment 15–20 minutes before testing. Baseline responses were determined on 3 different days using von Frey hairs, and the 50% paw withdrawal threshold was calculated using the up-and-down method (25, 69). In brief, animals were placed on a wire grid bottom through which the von Frey hairs were applied (bending force range, 0.02–1.4 g, starting with 0.16 g; Stoelting). The hair force was increased or decreased according to the response. Clear paw withdrawal, shaking, or licking were considered as nociceptive-like responses. Ambulation was considered an ambiguous response, and the stimulus was repeated in such cases.

Hyperalgesic priming and CFA models. To induce hyperalgesic priming, 5 μl carrageenan (1% in saline; Sigma-Aldrich) or 5 μl ΨεRACK (1 μg in saline; obtained from the W.M. Keck Facility of Yale University) (15) was intraplantarly injected into the hind paw. Control mice received 5 μl saline.

3–14 days later, mice received an intraplantar injection of 2.5 μl PGE_2 (40 μg/ml; Sigma-Aldrich), epinephrine (4 μg/ml; Sigma-Aldrich), 8-pCPT (5.04 μg/ml; Biolog LifeScience Institute), or 5 μl recombinant mouse IL-1β (200 ng/ml; R&D Systems) per paw. For the CFA model, 20 μl CFA (Sigma-Aldrich) was injected intraplantarly.

Immunohistochemical staining of GRK2. Mice were deeply anesthetized with sodium pentobarbital (50 mg/kg i.p.) and transcardially perfused with PBS followed by 4% paraformaldehyde, after which DRG (lumbar [L3–L5] and

thoracic [T6–T10]) and sciatic nerves were collected. Tissues were post-fixed, cryoprotected in sucrose, embedded in OCT compound, and frozen at –80°C. Frozen sections of DRG and sciatic nerve (10 μm) were stained with biotinylated IB4 (10 μg/ml; Vector Laboratories) and rabbit anti-GRK2 (1:100; Santa Cruz Biotechnology). Primary anti-GRK2 antibody blocked with a GRK2 blocking peptide (Santa Cruz Biotechnology) was used as a control. Staining was visualized with Alexa Fluor 488–conjugated streptavidin (1:200; Invitrogen) and Alexa Fluor 594–conjugated goat anti-rabbit antibody (1:200; Invitrogen) and photographed with an EVOS fl (AMG Life Technologies) using identical exposure times for all slides. GRK2 levels in $IB4^+$ and $IB4^-$ small-diameter DRG neurons (<23 μm diameter; ref. 70) and in sciatic nerve fibers were analyzed with NIH ImageJ.

The average background fluorescence for specific subsets of DRG neurons or sciatic nerves (primary GRK2 antibody plus GRK2 blocking peptide) were subtracted before calculation of the percent change in GRK2 staining. Stainings were done in parallel for samples from carrageenan-, ΨεRACK-, or CFA-treated mice and their respective saline-treated controls.

Western blotting. Lumbar and thoracic DRG were frozen in liquid nitrogen and homogenized in ice-cold 50 mM Tris-HCl (pH 8), 5 mM EDTA, 150 mM NaCl, 1% NP-40, 0.5% deoxycholic acid, 0.1% SDS containing protease inhibitor mix (Sigma-Aldrich), 100 mM PMSF, 10 mM β-glycerolphosphate, 1 mM $NaVO_3$, and 20 mM NaF.

Proteins were separated by 7.5% SDS-PAGE and transferred to polyvinylidene difluoride membranes (Millipore). Blots were stained with mouse anti-EPAC1 (Cell Signaling Technology), mouse anti-EPAC2 (Cell Signaling Technology), and goat anti-actin (Santa Cruz Biotechnology) followed by peroxidase-conjugated goat anti-mouse IgG plus IgM (heavy and light chain) (Jackson Immunoresearch) or peroxidase-conjugated donkey anti-goat IgG (Santa Cruz Biotechnology) and developed by enhanced chemiluminescence (GE Healthcare). Band density was determined using a GS-700 Imaging Densitometer (Bio-Rad).

HSV-mediated GRK2 and GFP gene expression. We generated a bicistronic HSV construct into which we cloned bovine *GRK2* or $GRK2^{K220R}$ under control of the α4 promotor and in which *GFP* expression is driven by the α22 promoter (34). Both are immediate early gene promoters and have similar kinetics of expression, so the reporter can reliably be used as an indicator of transgene expression (71, 72). Control HSV-*GFP* contains *GFP* under control of the α22 promoter only. Mice were inoculated intraplantarly twice with 2.5 μl of 1.4×10^7 pfu/ml. To control for *GRK2* and/or *GFP* expression, the unfixed skin of hind paws was isolated and frozen at day 3 after the last inoculation. In addition, fixed DRG and sciatic nerve tissues were prepared as described above.

Frozen sections of skin (14 μm) were fixed in acetone and stained with rabbit anti-GFP (1:100; GeneTex) for 60 hours and overnight at 4°C. Frozen sections of skin, DRG and sciatic nerve (10 μm) were incubated with rabbit anti-GFP (1:100; GeneTex) for 60 hours. Skin was stained with mouse anti-peripherin (1:100; Sigma-Aldrich); DRG and sciatic nerve was stained with IB4 (10 μg/ml; Vector Laboratories). We used Alexa Fluor 594–conjugated streptavidin (Invitrogen) and Alexa Fluor 488–conjugated donkey anti-rabbit antibody (Invitrogen) in the second step.

Epac1 and mismatch asODNs. The *Epac1* asODN sequence (5′-AACTCTC-CACCCTCTCCCA-3′) is directed against a unique sequence of mouse *Epac1* mRNA; mismatch asODN (5′-ACATTCCACCCTCCTCCAC-3′) was used as a control. 10 μg *Epac1* asODNs or mismatch asODNs in 5 μl saline were injected intrathecally between the fifth and sixth lumbar vertebrate under isoflurane anesthesia.

In situ hybridization. In situ hybridization for *Epac1* mRNA was performed on paraformaldehyde-fixed, paraffin-embedded tissue sections (4 μm). Sections were digested with 2 μg/ml proteinase K (Exiqon) for 5 minutes at room temperature and loaded onto Ventana Discovery Ultra for in situ hybridization analysis. Slides were incubated with double digoxigenin–labeled mercury LNA RNA probe specific for *Epac1* (5DigN/TGGAGCGGTATGAGTGTGAGT/3DigN; Exiqon) for 2 hours at 50°C. Slides were developed using a polyclonal anti-digoxegenin antibody and alkaline phosphatase–conjugated secondary antibody (Ventana) with NBT-BCIP as the substrate. A double digoxigenin–labeled probe specific for U6 small nuclear RNA (Exiqon) was used as positive control, and a double digoxigenin–labeled negative control probe (catalog no. 99004-15; Exiqon) was used as a negative control.

Statistics. Data are expressed as mean ± SEM. Statistical analysis was carried out using 2-tailed Student's *t* test or 2-way ANOVA followed by Bonferroni analysis. A *P* value less than 0.05 was considered significant.

Study approval. Mice were maintained in the animal facility of the University of Utrecht. All experiments were performed in accordance with international guidelines and approved by the University Medical Center Utrecht experimental animal committee.

Acknowledgments

The authors are indebted to Robert Sapolsky (Stanford University and Stanford University School of Medicine, Stanford, California, USA) for contributing to preparation of the HSV construct and scientific editor Jeanie F. Woodruff for expert editorial assistance. Research reported here was supported by the National Institute of Neurological Diseases and Stroke, NIH (award nos. RO1NS073939 and RO1NS074999). The content is solely the responsibility of the authors and does not necessarily represent the official views of the NIH. This research was also supported by a STARS grant of the University of Texas System to A. Kavelaars.

Received for publication May 13, 2013, and accepted in revised form September 12, 2013.

Address correspondence to: Annemieke Kavelaars, Neuroimmunology of Cancer Related Symptoms (NICRS) Laboratory, Department of Symptom Research, University of Texas M.D. Anderson Cancer Center, 1515 Holcombe Boulevard, Unit 1450, Houston, Texas 77030, USA. Phone: 713.794.5297; Fax: 713.743.3475; E-mail: akavelaars@mdanderson.org.

1. National Research Council. *Relieving Pain in America: A Blueprint for Transforming Prevention, Care, Education, and Research.* Washington, DC, USA: The National Academies Press; 2011.
2. Stein C, et al. Peripheral mechanisms of pain and analgesia. *Brain Res Rev.* 2009;60(1):90–113.
3. Gold MS, Gebhart GF. Nociceptor sensitization in pain pathogenesis. *Nat Med.* 2010;16(11):1248–1257.
4. Basbaum AI, Bautista DM, Scherrer G, Julius D. Cellular and molecular mechanisms of pain. *Cell.* 2009;139(2):267–284.
5. Woolf CJ. What is this thing called pain? *J Clin Invest.* 2010;120(11):3742–3744.
6. Latremoliere A, Woolf CJ. Central sensitization: a generator of pain hypersensitivity by central neural plasticity. *J Pain.* 2009;10(9):895–926.
7. Marchand F, Perretti M, McMahon SB. Role of the immune system in chronic pain. *Nat Rev Neurosci.* 2005;6(7):521–532.
8. Wallace MS, Irving G, Cowles VE. Gabapentin extended-release tablets for the treatment of patients with postherpetic neuralgia: a randomized, double-blind, placebo-controlled, multicentre study. *Clin Drug Investig.* 2010;30(11):765–776.
9. Aasvang E, Kehlet H. Chronic postoperative pain: the case of inguinal herniorrhaphy. *Br J Anaesth.* 2005;95(1):69–76.
10. Asiedu MN, et al. Spinal protein kinase M zeta underlies the maintenance mechanism of persistent nociceptive sensitization. *J Neurosci.* 2011; 31(18):6646–6653.
11. Melemedjian OK, et al. IL-6- and NGF-induced rapid control of protein synthesis and nociceptive plasticity via convergent signaling to the eIF4F complex. *J Neurosci.* 2010;30(45):15113–15123.
12. Geranton SM, et al. A rapamycin-sensitive signaling pathway is essential for the full expression of persistent pain states. *J Neurosci.* 2009;29(47):15017–15027.
13. Jimenez-Diaz L, et al. Local translation in primary

afferent fibers regulates nociception. *PLoS One*. 2008;3(4):e1961.
14. Obara I, Geranton SM, Hunt SP. Axonal protein synthesis: a potential target for pain relief? *Curr Opin Pharmacol*. 2012;12(1):42–48.
15. Aley KO, Messing RO, Mochly-Rosen D, Levine JD. Chronic hypersensitivity for inflammatory nociceptor sensitization mediated by the epsilon isozyme of protein kinase C. *J Neurosci*. 2000;20(12):4680–4685.
16. Joseph EK, Parada CA, Levine JD. Hyperalgesic priming in the rat demonstrates marked sexual dimorphism. *Pain*. 2003;105(1–2):143–150.
17. Reichling DB, Levine JD. Critical role of nociceptor plasticity in chronic pain. *Trends Neurosci*. 2009; 32(12):611–618.
18. Gloerich M, Bos JL. Epac: defining a new mechanism for cAMP action. *Annu Rev Pharmacol Toxicol*. 2010;50:355–375.
19. Kawasaki H, et al. A family of cAMP-binding proteins that directly activate Rap1. *Science*. 1998; 282(5397):2275–2279.
20. Hucho TB, Dina OA, Levine JD. Epac mediates a cAMP-to-PKC signaling in inflammatory pain: an isolectin B4(+) neuron-specific mechanism. *J Neurosci*. 2005;25(26):6119–6126.
21. Eijkelkamp N, et al. GRK2: a novel cell-specific regulator of severity and duration of inflammatory pain. *J Neurosci*. 2010;30(6):2138–2149.
22. Eijkelkamp N, et al. Low nociceptor GRK2 prolongs prostaglandin E2 hyperalgesia via biased cAMP signaling to Epac/Rap1, protein kinase Cepsilon, and MEK/ERK. *J Neurosci*. 2010;30(38):12806–12815.
23. Kavelaars A, Eijkelkamp N, Willemen HL, Wang H, Carbajal AG, Heijnen CJ. Microglial GRK2: a novel regulator of transition from acute to chronic pain. *Brain Behav Immun*. 2011;25(6):1055–1060.
24. Kleibeuker W, et al. A role for G protein-coupled receptor kinase 2 in mechanical allodynia. *Eur J Neurosci*. 2007;25(6):1696–1704.
25. Wang H, et al. GRK2 in sensory neurons regulates epinephrine-induced signalling and duration of mechanical hyperalgesia. *Pain*. 2011; 152(7):1649–1658.
26. Willemen HL, et al. Microglial/macrophage GRK2 determines duration of peripheral IL-1beta-induced hyperalgesia: contribution of spinal cord CX3CR1, p38 and IL-1 signaling. *Pain*. 2010;150(3):550–560.
27. Willemen HL, Huo XJ, Mao-Ying QL, Zijlstra J, Heijnen CJ, Kavelaars A. MicroRNA-124 as a novel treatment for persistent hyperalgesia. *J Neuroinflammation*. 2012;9:143.
28. Evron T, Daigle TL, Caron MG. GRK2: multiple roles beyond G protein-coupled receptor desensitization. *Trends Pharmacol Sci*. 2012;33(3):154–164.
29. Jimenez-Sainz MC, et al. G protein-coupled receptor kinase 2 negatively regulates chemokine signaling at a level downstream from G protein subunits. *Mol Biol Cell*. 2006;17(1):25–31.
30. Peregrin S, et al. Phosphorylation of p38 by GRK2 at the docking groove unveils a novel mechanism for inactivating p38MAPK. *Curr Biol*. 2006; 16(20):2042–2047.
31. Ferrari LF, Bogen O, Alessandri-Haber N, Levine E, Gear RW, Levine JD. Transient decrease in nociceptor GRK2 expression produces long-term enhancement in inflammatory pain. *Neuroscience*. 2012; 222:392–403.
32. Ferrari LF, Bogen O, Levine JD. Nociceptor subpopulations involved in hyperalgesic priming. *Neuroscience*. 2010;165(3):896–901.
33. Joseph EK, Levine JD. Hyperalgesic priming is restricted to isolectin B4-positive nociceptors. *Neuroscience*. 2010;169(1):431–435.
34. Zhao H, Yenari MA, Sapolsky RM, Steinberg GK. Mild postischemic hypothermia prolongs the time window for gene therapy by inhibiting cytochrome C release. *Stroke*. 2004;35(2):572–577.
35. Sallese M, Mariggio S, D'Urbano E, Iacovelli L, De Blasi A. Selective regulation of Gq signaling by G protein-coupled receptor kinase 2: direct interaction of kinase N terminus with activated galphaq. *Mol Pharmacol*. 2000;57(4):826–831.
36. Suzuki S, et al. Differential roles of Epac in regulating cell death in neuronal and myocardial cells. *J Biol Chem*. 2010;285(31):24248–24259.
37. Wang C, Gu Y, Li GW, Huang LY. A critical role of the cAMP sensor Epac in switching protein kinase signalling in prostaglandin E2-induced potentiation of P2X3 receptor currents in inflamed rats. *J Physiol*. 2007;584(pt 1):191–203.
38. Eijkelkamp N, et al. A role for Piezo2 in EPAC1-dependent mechanical allodynia. *Nat Commun*. 2013;4:1682.
39. Ferrari LF, Bogen O, Chu C, Levine JD. Peripheral administration of translation inhibitors reverses increased hyperalgesia in a model of chronic pain in the rat. *J Pain*. 2013;14(7):731–738.
40. Misra UK, Pizzo SV. Upregulation of mTORC2 activation by the selective agonist of EPAC, 8-CPT-2Me-cAMP, in prostate cancer cells: assembly of a multiprotein signaling complex. *J Cell Biochem*. 2012;113(5):1488–1500.
41. Misra UK, Pizzo SV. Epac1-induced cellular proliferation in prostate cancer cells is mediated by B-Raf/ERK and mTOR signaling cascades. *J Cell Biochem*. 2009;108(4):998–1011.
42. Lombardi MS, et al. Decreased expression and activity of G-protein-coupled receptor kinases in peripheral blood mononuclear cells of patients with rheumatoid arthritis. *FASEB J*. 1999;13(6):715–725.
43. Vroon A, et al. G protein-coupled receptor kinase 2 in multiple sclerosis and experimental autoimmune encephalomyelitis. *J Immunol*. 2005; 174(7):4400–4406.
44. Lombardi MS, Kavelaars A, Cobelens PM, Schmidt RE, Schedlowski M, Heijnen CJ. Adjuvant arthritis induces down-regulation of G protein-coupled receptor kinases in the immune system. *J Immunol*. 2001;166(3):1635–1640.
45. Vroon A, Lombardi MS, Kavelaars A, Heijnen CJ. Changes in the G-protein-coupled receptor desensitization machinery during relapsing-progressive experimental allergic encephalomyelitis. *J Neuroimmunol*. 2003;137(1–2):79–86.
46. Gerke MB, Plenderleith MB. Binding sites for the plant lectin Bandeiraea simplicifolia I-isolectin B(4) are expressed by nociceptive primary sensory neurones. *Brain Res*. 2001;911(1):101–104.
47. Lagerstrom MC, et al. A sensory subpopulation depends on vesicular glutamate transporter 2 for mechanical pain, and together with substance P, inflammatory pain. *Proc Natl Acad Sci U S A*. 2011; 108(14):5789–5794.
48. Minett MS, et al. Distinct Nav1.7-dependent pain sensations require different sets of sensory and sympathetic neurons. *Nat Commun*. 2012;3:791.
49. Wood JN, Eijkelkamp N. Noxious mechanosensation — molecules and circuits. *Curr Opin Pharmacol*. 2012;12(1):4–8.
50. Breese NM, George AC, Pauers LE, Stucky CL. Peripheral inflammation selectively increases TRPV1 function in IB4-positive sensory neurons from adult mouse. *Pain*. 2005;115(1–2):37–49.
51. Stemkowski PL, Smith PA. Long-term IL-1beta exposure causes subpopulation-dependent alterations in rat dorsal root ganglion neuron excitability. *J Neurophysiol*. 2012;107(6):1586–1597.
52. Abrahamsen B, et al. The cell and molecular basis of mechanical, cold, and inflammatory pain. *Science*. 2008;321(5889):702–705.
53. Henken DB, Martin JR. Herpes simplex virus infection in populations of mouse dorsal root ganglion neurons: effects of inoculation route and virus strain. *J Neurol Sci*. 1991;105(1):29–36.
54. Chuang TT, Sallese M, Ambrosini G, Parruti G, De Blasi A. High expression of beta-adrenergic receptor kinase in human peripheral blood leukocytes. Isoproterenol and platelet activating factor can induce kinase translocation. *J Biol Chem*. 1992; 267(10):6886–6892.
55. Grange-Midroit M, Garcia-Sevilla JA, Ferrer-Alcon M, La Harpe R, Walzer C, Guimon J. G protein-coupled receptor kinases, beta-arrestin-2 and associated regulatory proteins in the human brain: postmortem changes, effect of age and subcellular distribution. *Brain Res Mol Brain Res*. 2002;101(1–2):39–51.
56. Monto F, et al. Different expression of adrenoceptors and GRKs in the human myocardium depends on heart failure etiology and correlates to clinical variables. *Am J Physiol Heart Circ Physiol*. 2012; 303(3):H368–H376.
57. Harris DM, Cohn HI, Pesant S, Eckhart AD. GPCR signalling in hypertension: role of GRKs. *Clin Sci (Lond)*. 2008;115(3):79–89.
58. Premont RT, Gainetdinov RR. Physiological roles of G protein-coupled receptor kinases and arrestins. *Annu Rev Physiol*. 2007;69:511–534.
59. Hutchinson MR, et al. Low-dose endotoxin potentiates capsaicin-induced pain in man: evidence for a pain neuroimmune connection. *Brain Behav Immun*. 2013;30:3–11.
60. Poobalan AS, Bruce J, King PM, Chambers WA, Krukowski ZH, Smith WC. Chronic pain and quality of life following open inguinal hernia repair. *Br J Surg*. 2001;88(8):1122–1126.
61. Callesen T, Bech K, Kehlet H. Prospective study of chronic pain after groin hernia repair. *Br J Surg*. 1999;86(12):1528–1531.
62. Dai C, Jiang M. The incidence and risk factors of post-infectious irritable bowel syndrome: a meta-analysis. *Hepatogastroenterology*. 2012;59(113):67–72.
63. Lomholt JJ, Thastum M, Herlin T. Pain experience in children with juvenile idiopathic arthritis treated with anti-TNF agents compared to non-biologic standard treatment. *Pediatr Rheumatol Online J*. 2013;11(1):21.
64. Kimura Y, Walco GA. Treatment of chronic pain in pediatric rheumatic disease. *Nat Clin Pract Rheumatol*. 2007;3(4):210–218.
65. Wolfe D, Mata M, Fink DJ. Targeted drug delivery to the peripheral nervous system using gene therapy. *Neurosci Lett*. 2012;527(2):85–89.
66. Goins WF, Cohen JB, Glorioso JC. Gene therapy for the treatment of chronic peripheral nervous system pain. *Neurobiol Dis*. 2012;48(2):255–270.
67. Fink DJ, et al. Gene therapy for pain: results of a phase I clinical trial. *Ann Neurol*. 2011;70(2):207–212.
68. Cheli VT, et al. Gene transfer of NMDAR1 subunit sequences to the rat CNS using herpes simplex virus vectors interfered with habituation. *Cell Mol Neurobiol*. 2002;22(3):303–314.
69. Chaplan SR, Bach FW, Pogrel JW, Chung JM, Yaksh TL. Quantitative assessment of tactile allodynia in the rat paw. *J Neurosci Methods*. 1994;53(1):55–63.
70. Fang X, et al. Intense isolectin-B4 binding in rat dorsal root ganglion neurons distinguishes C-fiber nociceptors with broad action potentials and high Nav1.9 expression. *J Neurosci*. 2006;26(27):7281–7292.
71. Fink SL, Chang LK, Ho DY, Sapolsky RM. Defective herpes simplex virus vectors expressing the rat brain stress-inducible heat shock protein 72 protect cultured neurons from severe heat shock. *J Neurochem*. 1997;68(3):961–969.
72. Yenari MA, et al. Gene therapy with HSP72 is neuroprotective in rat models of stroke and epilepsy. *Ann Neurol*. 1998;44(4):584–591.

Am J Physiol Heart Circ Physiol 305: H1–H8, 2013.
First published April 26, 2013; doi:10.1152/ajpheart.00080.2013.

Review

Adenylyl cyclase type 5 in cardiac disease, metabolism, and aging

Stephen F. Vatner,[1]* Misun Park,[1]* Lin Yan,[1] Grace J. Lee,[1] Lo Lai,[1] Kousaku Iwatsubo,[1] Yoshihiro Ishikawa,[1] Jeffrey Pessin,[2] and Dorothy E. Vatner[3]

[1]*Department of Cell Biology and Molecular Medicine, and the Cardiovascular Research Institute at the University of Medicine and Dentistry of New Jersey, New Jersey Medical School, Newark, New Jersey;* [2]*Department of Medicine, and Diabetes Research Center, Albert Einstein College of Medicine, Bronx, New York; and* [3]*Department of Medicine, and the Cardiovascular Research Institute at the University of Medicine and Dentistry of New Jersey, New Jersey Medical School, Newark, New Jersey*

Submitted 29 January 2013; accepted in final form 11 April 2013

Vatner SF, Park M, Yan L, Lee GJ, Lai L, Iwatsubo K, Ishikawa Y, Pessin J, Vatner DE. Adenylyl cyclase type 5 in cardiac disease, metabolism, and aging. *Am J Physiol* Heart Circ Physiol 305: H1–H8, 2013. First published April 26, 2013; doi:10.1152/ajpheart.00080.2013.—G protein-coupled receptor/adenylyl cyclase (AC)/cAMP signaling is crucial for all cellular responses to physiological and pathophysiological stimuli. There are nine isoforms of membrane-bound AC, with type 5 being one of the two major isoforms in the heart. Since the role of AC in the heart in regulating cAMP and acute changes in inotropic and chronotropic state are well known, this review will address our current understanding of the distinct regulatory role of the AC5 isoform in response to chronic stress. Transgenic overexpression of AC5 in cardiomyocytes of the heart (AC5-Tg) improves baseline cardiac function but impairs the ability of the heart to withstand stress. For example, chronic catecholamine stimulation induces cardiomyopathy, which is more severe in AC5-Tg mice, mediated through the AC5/sirtuin 1/forkhead box O3a pathway. Conversely, disrupting AC5, i.e., AC5 knockout, protects the heart from chronic catecholamine cardiomyopathy as well as the cardiomyopathies resulting from chronic pressure overload or aging. Moreover, AC5 knockout results in a 30% increase in a healthy life span, resembling the most widely studied model of longevity, i.e., calorie restriction. These two models of longevity share similar gene regulation in the heart, muscle, liver, and brain in that they are both protected against diabetes, obesity, and diabetic and aging cardiomyopathy. A pharmacological inhibitor of AC5 also provides protection against cardiac stress, diabetes, and obesity. Thus AC5 inhibition has novel, potential therapeutic applicability to several diseases not only in the heart but also in aging, diabetes, and obesity.

adenylyl cyclase type 5; cardiomyopathy; aging; metabolism; AC5 inhibitor

THIS ARTICLE is part of a collection on **G Protein Kinase A Signaling in Cardiovascular Physiology and Disease.** Other articles appearing in this collection, as well as a full archive of all collections, can be found online at http://ajpheart.physiology.org/.

Adenylyl cyclase (AC) is the enzyme that catalyzes the conversion of ATP to adenosine 3′,5′-cyclic monophosphate (cAMP), a key intracellular second messenger, which in the heart mediates inotropy and chronotropy. Since the pioneering work 55 years ago by Sutherland (73), it has been known that AC-cAMP signaling plays crucial roles in normal biological function, for example, lipolysis (53), gluconeogenesis (54), respiration (29) and cytoskeletal organization (25), and its dysregulation in pathophysiological states including memory (52) and neurodegenerative disorders (69), tumorigenesis (66), and heart disease (13, 19). The diverse actions of cAMP are mediated through the cAMP-dependent activation of protein kinase A (PKA), cyclic nucleotide-gated ion channels, and cAMP-activated exchange proteins. Ten different isoforms of ACs have been identified in mammalian tissues; nine are G protein-regulated transmembrane ACs, and one is a soluble form of AC (9). Each of the various isoforms has a unique chromosomal distribution (28), indicating that there is a significant heterogeneity in the distribution and biochemical properties within AC isoforms. The overall amino acid similarity between the different AC isoforms is ~60%. Although all the AC isoforms are ubiquitously expressed, each is characterized by distinct biochemical properties, differential regulatory roles, and tissue-specific distribution throughout the body. Local increases in cAMP derived from tissue-specific isoforms of ACs can selectively regulate closely associated proteins, providing possibilities for different cells to respond diversely to similar stimuli. Thus the AC isoforms are subclassified according to their regulation by various endogenous modulators such as calcium/calmodulin and protein kinase C (PKC) and PKA feedback phosphorylation.

The membrane-bound ACs (AC1–AC9) are large proteins (~120–140 kDa) that share a common structure consisting of

* S. F. Vatner and M. Park are co-first authors.
Address for reprint requests and other correspondence: S. F. Vatner, Dept. of Cell Biology and Molecular Medicine, New Jersey Medical School, Univ. of Medicine and Dentistry of New Jersey, 185 S. Orange Ave., MSB G-609, Newark, NJ 07103 (e-mail: vatnersf@umdnj.edu).

an intracellular NH_2-terminus, two repeats of six transmembrane domains (M1 and M2) and two cytoplasmic catalytic domains of ~40 kDa each (C1 and C2). Crystal structure-coupled with biochemical data indicate that two cytosolic domains form the catalytic core pocket, and ATP binds at one of two pseudosymmetric binding sites at the C1-C2 interface (10, 75). Forskolin binds in two almost equivalent pockets at either end of C1 and C2 domains (87). For the isoforms of AC1, AC2, and AC5, expression of either the α-half (M1/C1) or the β-half (M2/C2) of the molecule alone is insufficient to generate enzymatic activity. The specificity of AC response likely depends on the creation of intracellular microdomains containing signaling molecules. In the submicromolar range of Ca^{2+}, the sensitivity of ACs for Ca^{2+} is coupled with distinct subcellular localization of Ca^{2+}-sensitive AC isoforms (82, 83), suggesting a temporally and spatially distinct pattern of cAMP signaling, depending on the localization of ACs in Ca^{2+} microdomains within the plasma membrane or cytoplasm. For instance, studies in overexpression models suggested that AC8 may augment cardiac contractility by preferentially activating Ca^{2+} loading of sarcoplasmic reticulum through cAMP compartmentation, rather than enhancing Ca^{2+} influx via L-type Ca^{2+} channels (21). Dyachok et al. (12) suggested that oscillations of cAMP lead to selective target activation by restricting the spatial redistribution of PKA (12). β-Adrenergic receptors (β-AR) are selectively located in plasma membrane lipid raft microdomains, resulting in more efficient coupling to AC compared with nonlipid raft microdomain receptors, such as the E-prostanoid-2 receptor. Signaling modules that include AC isoforms also contain A kinase anchoring proteins (AKAPs), PKA, and anchored phosphodiesterases to provide microdomains of cAMP production and signaling (2, 34, 82, 86).

Since AC signaling in general and AC5 signaling in particular have been extensively reviewed (31, 56, 67), this review will focus on AC5 and its regulation of responses to chronic stress and disease. We will also provide a brief overview of the potential translational direction of this work, discussing some of our recent findings with a pharmacological AC5 inhibitor.

β-AR-G Protein-AC-cAMP Signaling Pathway

The β-AR-G protein-AC-cAMP signaling pathway is one of the major pathophysiological mechanisms for regulation of cardiac function (31, 45, 47, 78). By targeting Ca^{2+} handling proteins, it provides strong inotropic and chronotropic response in times of need, such as in fight or flight (22, 48, 70, 72). Throughout much of the 20th century, it was believed that stimulation of this pathway could provide inotropic support and should be used in heart failure therapy. It was shown that transgenic (Tg) mice with up to 60-fold overexpression of β_2-AR had enhanced cardiac function without signs of cardiac pathology (46, 51). Furthermore, β_2-AR transgene experiments showed improvement in function in failing rabbit hearts (76). More recent work with adenoviral-mediated β_2-AR transgene overexpression demonstrated enhanced cardiac function in a rat model of heart failure (65). However, the concept of treating heart failure with chronically enhanced β-AR stimulation became controversial when patients responded positively to acute β-AR inotropic therapy, particularly with dopamine and dobutamine, but had poor outcomes when on prolonged inotropic therapy (14, 44, 55). An experimental study that first highlighted the adverse effects of chronic β-AR signaling was shown in $G_{s\alpha}$ Tg mice (36). Although these animals had higher responsiveness to isoproterenol (Iso) when young, a picture of cardiomyopathy developed as they aged, including myocardial hypertrophy, fibrosis and necrosis, and depression of cardiac function (1, 36, 37). Later studies using β_1-AR (15, 16, 63)- and β_2-AR (11, 63)-overexpressed models confirmed these findings, i.e., hyperfunction at young age and deterioration of function with aging. These studies (1, 11, 15, 16, 36, 37, 63) in combination with clinical studies showing poor outcomes in patients on β-AR agonists (14, 44, 55) and Bristow's classical study in *The New England Journal of Medicine* demonstrating desensitization of the β-AR in patients with heart failure (4) changed the paradigm from treating patients with heart failure with β-AR agonists to antagonists (7, 8, 30, 60, 68). Heart failure still remains as the leading cause of mortality and morbidity in the United States. For this reason, targeting components distal to the β-AR signaling, such as ACs, will be important for the development of future treatment of heart failure.

AC in the Heart

Whereas AC2, -3, -4, -5/6, and -7 are detected in rat cardiac fibroblasts (59), AC5 and AC6 are the two major isoforms expressed in the adult mammalian heart (23, 35). Both AC5 and AC6 regulate heart rate and contractility, but AC6 plays a more significant role at baseline in view of the relatively minor reduction in AC content and corresponding reductions in cardiac contractility observed in AC5 knockout (AC5-KO) hearts (58). However, the role of these two major isoforms in the heart in mediating the response to cardiac stress is controversial. In this article, we first review the studies demonstrating an adverse effect of overexpression of AC5 and beneficial effects of disrupting AC5 on cardiomyopathies induced by chronic Iso stimulation, aging, and pressure overload in either AC5-Tg or AC5-KO mice. This leads to a discussion of other factors involved in AC5 protection against aging, e.g., metabolism and diabetes. Since not all studies are in agreement, we then discuss those with an opposite point of view and reconcile the differences. The controversial studies on AC6 overexpression and disruption are beyond the scope of this review, which focuses on AC5.

Regulation of Cardiomyopathy by AC5

Chronic catecholamine cardiomyopathy. Chronic Iso increased oxidative stress and induced a more severe cardiomyopathy in AC5-Tg compared with wild-type (WT) mice, as reflected by a greater impairment of left ventricular (LV) ejection fraction (EF) along with greater LV dilation and increased fibrosis, apoptosis, and hypertrophy (41) (Fig. 1, *A* and *B*). LV EF fell more ($P < 0.05$) in AC5-Tg than WT mice (-35 ± 2 vs. $-18 \pm 1\%$). Oxidative stress induced by chronic Iso was greater in AC5-Tg hearts, whereas protein expression of manganese superoxide dismutase (MnSOD), which protects against oxidative stress, was reduced by 36%, suggesting that the increased severity of the cardiomyopathy in AC5-Tg may have resulted as a consequence of decreased MnSOD expression. This was confirmed by mating AC5-Tg with MnSOD-Tg mice. These bigenic mice no longer responded to chronic Iso with more severe cardiomyopathy than WT mice. In fact, LV EF fell less in AC5-Tg × MnSOD-Tg ($-13 \pm 1\%$) versus either AC5-Tg or WT mice. LV EF fell similarly in

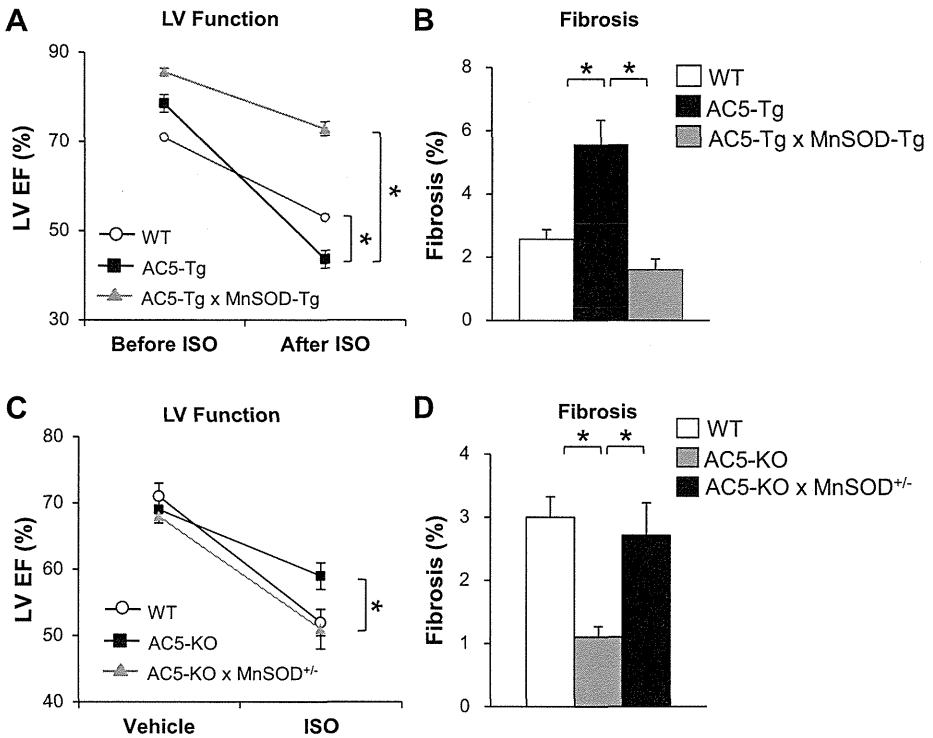

Fig. 1. *A* and *B*: chronic isoproterenol (Iso) exacerbated cardiomyopathy in transgenic overexpression of adenylyl cyclase 5 in cardiomyocytes of the heart (AC5-Tg) compared with wild-type (WT), and the cardiomyopathy was rescued by mating the AC5-Tg mice with MnSOD-Tg (AC5-Tg × MnSOD-Tg) mice (41). *C* and *D*: downregulation of MnSOD eliminated the protective effects of AC5-knockout (KO) with chronic Iso. LV, left ventricular; EF, ejection fraction. $*P < 0.05$ (41). Figures used are modified with permission from Lai et al. (41).

MnSOD-Tg alone (−13 ± 2%). Conversely, AC5-KO mice are protected from the cardiomyopathy induced by chronic Iso treatment (58), as reflected by less of a reduction with chronic Iso ($P < 0.05$) in AC5-KO than WT (−10 ± 2 vs. −19 ± 2%) mice, and this protection was lost in bigenic AC5-KO mice mated with MnSOD heterozygous KO mice, where LV EF fell by −18 ± 3% (Fig. 1, *C* and *D*). The decrease in LV EF with chronic Iso in the bigenic AC5-KO × MnSOD heterozygous mouse was similar to that in the MnSOD heterozygous alone (−18 ± 3 vs. −18 ± 4%). The decreases in LV EF must be interpreted with the histological changes in the heart consistent with chronic cardiomyopathy, e.g., fibrosis and apoptosis. When the data are all taken together, the picture of intensification of cardiomyopathy with AC5-Tg and protection with MnSOD-Tg or AC5-KO becomes even more apparent. We also demonstrated that AC5, but not AC6, regulates MnSOD at the transcriptional level via the sirtuin 1/forkhead box O3a pathway (Fig. 2). Thus the cardiomyopathy induced by chronic catecholamine stress is intensified in AC5-Tg by inhibiting sirtuin 1/forkhead box O3a, which downregulates MnSOD transcription, resulting in oxidative stress intolerance (41).

Chronic pressure-overload cardiomyopathy. Cardiac hypertrophy in response to pressure overload is a double- edged sword; on the one-hand it compensates for the pressure overload, whereas on the other hand LV hypertrophy impairs LV function (26, 40), eventually leading to heart failure. AC5-KO mice tolerated chronic pressure overload better than WT, with improved LV function, less fibrosis, and apoptosis in the heart (57).

We previously showed that AC5 and AC6 have opposite protein expression levels in response to pressure overload LV hypertrophy, e.g., an upregulation of AC5 and a downregulation of AC6 (33), suggesting unique regulatory pathways for AC5 in response to chronic pressure overload cardiomyopathy. In addition, it was reported that myocardial AC5 mRNA expression was increased from 5–12 wk in spontaneously hypertensive rats, which was accompanied by development of LV hypertrophy and hypertension (20). Recently, from mi-

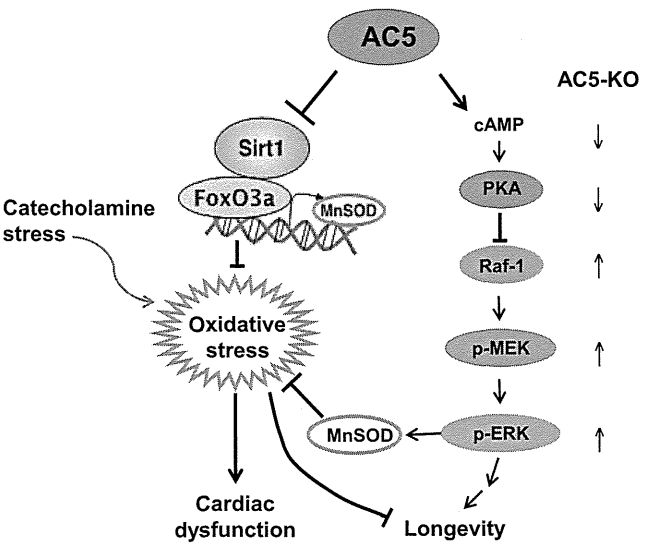

Fig. 2. Signaling diagram for AC5 mediating cardiac stress and longevity. *Left*: cardiac dysfunction: signaling diagram for AC5 regulation of MnSOD transcriptionally through the sirtuin 1/forkhead box O3a (SIRT1/FoxO3a) pathway is shown. Imbalance between reactive oxygen species production and the intracellular antioxidant system results in the intolerance of AC5-Tg to stress (41). *Right*: longevity: disruption of AC5 activates the Raf/MEK/ERK signaling pathway. The activation of ERK activates antioxidative stress and cell survival mechanism, which leads to longevity in AC5-KO mice (85). Arrows indicate the direction of signaling. Figures used are modified with permission from Lai et al. (41) and Yan et al. (85).

croarray analysis we found several genes in AC5-Tg hearts related to LV hypertrophy, which was similar to those in a public data set for pressure overload LV hypertrophy and that the transcription factor binding site of nuclear factor of activated t-cells (NFAT), a key prohypertrophic pathway (3, 81), is enriched in AC5-Tg hearts even at baseline, suggesting that cardiac overexpression of AC5 predisposes the heart to LV hypertrophy (61), which is not observed in AC6-Tg hearts (27). Another mechanism mediating the role of AC5 and hypertrophy is the muscle protein AKAP (mAKAPβ), which is required for the cAMP second messenger controlling cardiac myocyte hypertrophy. AC5 binds selectively and directly to a unique NH_2-terminal site on mAKAPβ, but not AC6 (39).

Aging cardiomyopathy. The genetically engineered mouse model in which type 5 AC was knocked out, i.e., AC5-KO mice, have increased median life span of ~30% (Fig. 3*A*) and are protected from aging-induced cardiomyopathy (85), including decreased LV hypertrophy, decreased fibrosis, and decreased apoptosis compared with WT as they age (Fig. 3*B*). Using a proteomic-based approach, we demonstrated a significant activation of the Raf/MEK/ERK signaling pathway, which results in protection from oxidative stress, leading to longevity in AC5-KO mice (Fig. 2). In addition to the prolonged life and protection against aging cardiomyopathy in AC5-KO mice, this model also exhibits protection against the osteoporosis of aging (85). Furthermore, both young and old AC5-KO mice had better exercise endurance than WT mice of the corresponding age. These beneficial effects of AC5 disruption on aging are synergistic in clinical relevance of AC5 inhibition, since elderly patients have an increased prevalence of heart failure (42, 43).

AC5-KO model vs. calorie restriction models of longevity. Calorie restriction (CR) is the most widely studied model of longevity (5, 50, 71). Our hypothesis was that superimposing CR on the AC5-KO would combine their potentially different mechanisms mediating longevity resulting in a superlongevity model. This hypothesis was not correct, and superimposing CR on the AC5-KO was uniformly lethal within a month (79, 84). AC5-KO mice on CR developed a syndrome similar to starvation, as evidenced by greater decrease in body weight, blood glucose, fat and glycogen storage, and greater increase in ketone bodies than either AC5-KO or CR alone. Accordingly, we adopted the converse hypothesis that the longevity mechanisms were similar in the two models. To test this, we recently compared AC5-KO model with CR in terms of physical phenotype as well as metabolic and gene expression profiles (84). Similar to the mice on CR, AC5-KO mice exhibit a lower body weight, reduced fat accumulation (Fig. 4*B*) and glycogen stores, and lower fasting blood glucose levels. However, in contrast to CR with restricted food intake, AC5-KO mice eat more compared with their WT littermates. Microarray analysis revealed a remarkable similarity of gene profiles between AC5-KO and CR mice in the heart, skeletal muscle, and brain (Fig. 4*A*). Many tissue-specific pathways in the regulation of metabolism, longevity, and stress resistance overlap in the AC5-KO and CR mouse models, including sensory perception in heart and brain, muscle function in skeletal muscle, and lipid metabolism in liver (Fig. 4*C*). Importantly, the similarly regulated genes and pathways for AC5-KO and CR will begin to establish a unified theory for longevity, stress resistance, and potentially for diabetes and obesity.

Diabetic cardiomyopathy. A key extrapolation from the above study comparing AC5-KO and CR is that both models of longevity protect against glucose intolerance and insulin resistance (24, 32, 80, 84) and, taken together with AC5-KO's ability to protect against pressure overload and catecholamine cardiomyopathy, raises the likely probability that AC5-KO also might protect against diabetic cardiomyopathy. Even at

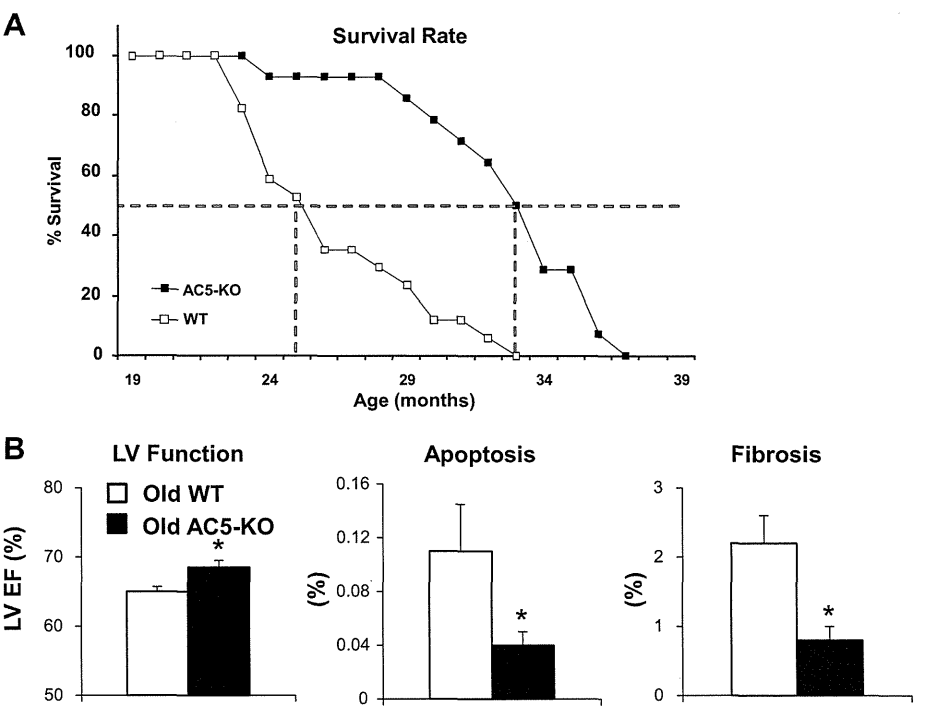

Fig. 3. Disruption of AC5 protects against cardiac stress. *A*: effects of AC5-KO on longevity (85). *B*: effects of AC5-KO on aging cardiomyopathy. LV EF, apoptosis, and fibrosis were significantly different in old AC5-KO vs. old WT. $*P < 0.05$. Figures used are modified with permission from Yan et al. (85).

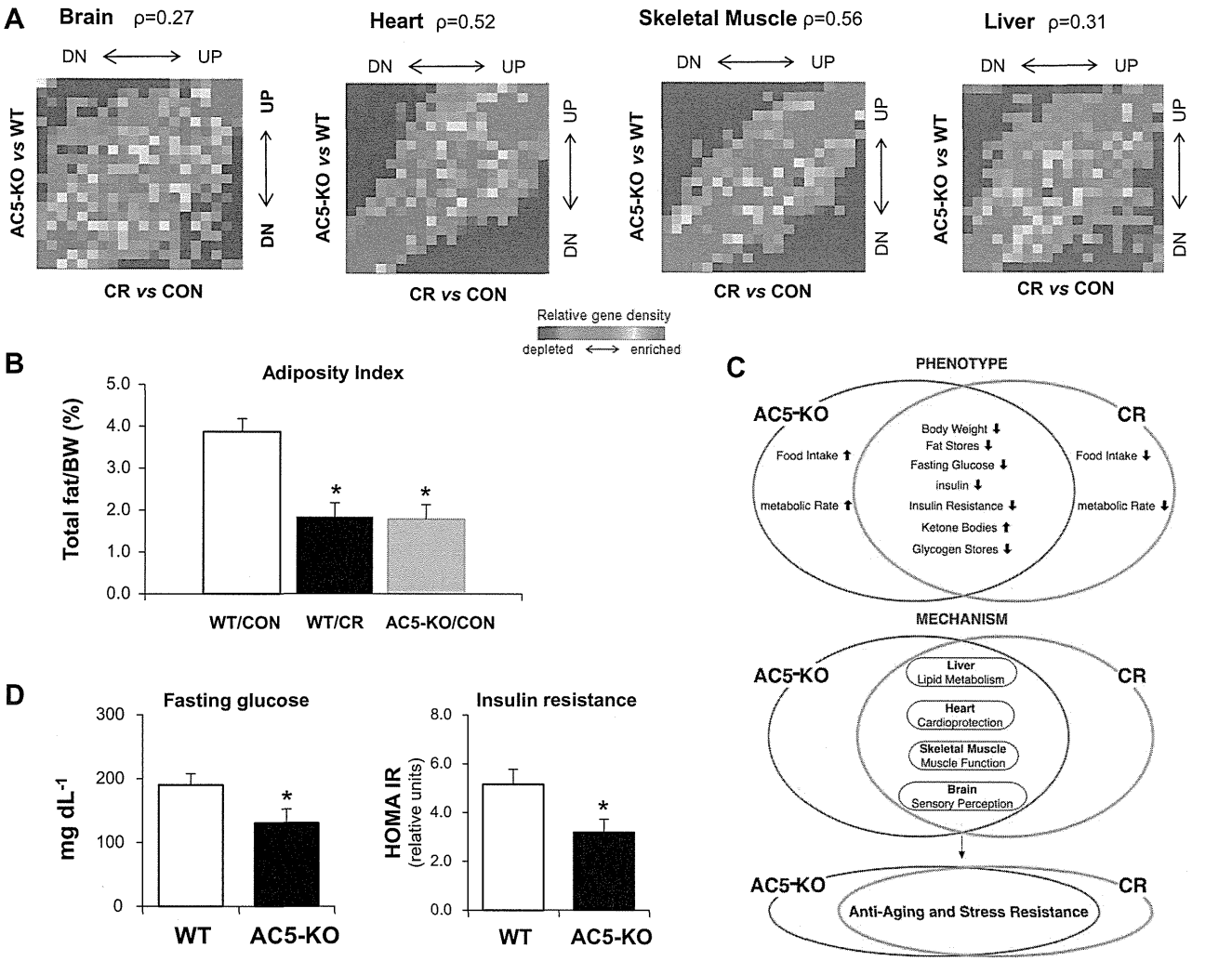

Fig. 4. Common mechanisms for calorie restriction (CR) and AC5-KO models. *A*: microarray analysis revealed a similarity between the changes in gene expression between AC5-KO and CR mice. Con, control diet; DN, down; UP, up (84). *B*: adiposity index showed that AC5-KO mice have less fat accumulation. WT/Con, WT on control diet; WT/CR, WT on calorie restriction; AC5-KO/CON, AC5-KO on control diet. $*P < 0.05$ (84). BW, body weight. *C*: differences and similarities between AC5-KO and CR mice are shown in the metabolic phenotypes and the common mechanisms regarding resistance to aging and stress (84). *D*: fasting glucose level and insulin resistance of AC5-KO and WT following 6 h fasting. ; BW, body weight; HOMA IR, homeostasis model of assessment-insulin resistance. $*P < 0.05$ (84). Figure used is modified with permission from Yan et al. (84).

baseline, in the absence of a high-fat diet, levels of fasting glucose and insulin resistance were lower in AC5-KO (Fig. 4*D*). Our preliminary results suggest that AC5-KO protects against diabetic cardiomyopathy (32). When the AC5-KO and their WT were placed on a high-fat diet, the WT rapidly developed a reduction in cardiac function with histopathological evidence of cardiomyopathy, as typically reported in the literature (6, 18, 62). However, the AC5-KO was protected against high-fat diet-induced cardiomyopathy (32). These observations underlie several important and clinical relevant questions. For example, is the protection of the cardiomyopathy due to an action of AC5-KO on the heart, i.e., the target organ of the cardiomyopathy, or is it indirectly due to an action on metabolism, i.e., the initiating cause of the cardiomyopathy? These and other related investigations are currently underway.

Controversy in role of AC5 in the heart. Not all studies have found that overexpression of AC5 is deleterious or that its disruption is salutary. For example, when AC5 is overexpressed in the heart, LV function is improved as well as the response to exercise (17). This is not particularly surprising since increasing any component of the β-AR signaling pathway, even at the level of the β-receptor, improves cardiac performance at baseline and in the response to exercise, as we have also observed in our AC5-Tg models. The adverse effects appear much later with chronically enhanced β-AR signaling. The bottom line is that patients with heart failure respond favorably to β-AR blockade over the long haul but have increased mortality with chronically enhanced β-AR stimulation. A more controversial finding is that AC5-Tg was able to rescue $G_{\alpha q}$ overexpression-induced cardiomyopathy (74) but not cardiomyopathy induced by cardiac overexpression of β-AR (64). Conversely, AC5-KO mice were not able to rescue $G_{\alpha q}$ overexpression-induced cardiomyopathy (77). These seemingly different results from rescue of cardiomyopathy (57,

58, 77) are not likely due to different backgrounds in the KO mice, but rather reconciliation of the differences in these studies is more apparent when understanding the signaling pathways. For example, Tg mice with cardiac-specific overexpression of $G_{\alpha q}$ showed that the cardiomyopathy was mediated by PKC with a significant reduction in AC5. Therefore, it is logical that replacing AC5 in this situation would be beneficial and that reducing it further, as with the AC5-KO, would not be beneficial. However, β_1-AR or chronic Iso-stimulated cardiomyopathy is mediated by PKA with increased levels of AC5 (58). These results, taken together, support our hypothesis that chronically elevated levels of AC activation, like β-AR (11, 16, 63) or $G_{s\alpha}$ (1, 36, 37), are deleterious and facilitate development of cardiomyopathy. In contrast, when a cardiomyopathy develops associated with reduced levels of AC5, restoration of AC5 expression may be beneficial for normal cardiac function under these conditions.

Clinical Relevance of AC5

Although hundreds, if not thousands, of novel and exciting discoveries have been made by alterations in genes in genetically engineered mice, relatively few have translated into improving clinical care. One reason for the lack of success is that it is difficult to overexpress or delete a gene in patients. Therefore, the goal becomes to have a pharmacological analog of the altered gene that can be safely delivered to patients. A current goal of our laboratory is to translate the beneficial effects of the AC5-KO model to clinical therapy. In this connection, while screening for a commercially available drug for the AC5 inhibition, adenine-9-β-D-arabinofuranoside (Ara-A; Vidarabine) showed a selective inhibition of AC5. Recent studies in our laboratory demonstrated that Ara-A selectively inhibits AC5 activity in AC5-Tg mice, but not in AC6-Tg mice. In cardiac membrane preparations with Iso stimulation, Ara-A (10 μM) reduced cAMP production much more in AC5-Tg (49%) than in WT and not at all in AC5-KO (38). Ara-A was originally developed as an antiviral drug, which was approved by the United States Food and Drug Administration. It has been clinically used for treatment of herpes virus infection, but it was found to be less efficient for viral therapy than the newer drug, acyclovir. We also found that this pharmacological AC5 inhibitor recapitulates the favorable effects of AC5 disruption and ameliorated the development of cardiomyopathy and heart failure induced by either permanent coronary artery occlusion or chronic catecholamine infusion (38). Ara-A significantly improved the survival rate and LV function compared with vehicle after 3 wk of coronary artery occlusion, and these beneficial effects of Ara-A were abolished by U0126, a MEK inhibitor, suggesting the involvement of the downstream MEK-ERK pathway of AC5 (38). This is significant since the same signaling pathway was found mediating the longevity in AC5-KO (85). In heart failure, Ara-A has also been shown to reduce autophagy by inhibition of AMPK (49). Since toxicology for the drug has found little to be contraindicated in heart failure and since adverse effects were only manifest with very high chronic doses, low dose Ara-A is a strong candidate for a clinical trial for heart failure since it selectively inhibits AC5, has been shown to protect against heart failure without adverse effects, and has been already approved by the United States Food and Drug Administration. One potential limitation to this drug is that only an intravenous formulation is currently available. Accordingly, drug discovery studies will have to be pursued for oral delivery and optimizing the compound for heart failure applications.

Conclusions

There are several take-home messages. First, although AC5 and AC6 are the two major isoforms in the heart, they mediate dramatically different functions, particularly in response to stress. Second, although AC5 is one of the major cardiac isoforms of AC, potentially its most important role will be in mediating diabetes, obesity, and longevity, even more so than in cardiac protection. Finally, it may be possible to translate the beneficial effects of the AC5-KO to the bedside, by using a pharmacological analog, which preferentially inhibits AC5.

GRANTS

This study was supported by National Institutes of Health Grants HL-093481, HL-106511, HL-033107, HL-095888, HL-069020, and AG-027211.

DISCLOSURES

S. F. Vatner and D. E. Vatner both work for Vasade Biosciences, which also has research interests in AC5 but has no intellectual property and did not provide support for this study. All research was funded by the NIH.

AUTHOR CONTRIBUTIONS

S.F.V. and D.E.V. conception and design of research; S.F.V., M.P., and L.Y. drafted manuscript; S.F.V., M.P., G.J.A.L., L.L., K.I., Y.I., J.E.P., and D.E.V. edited and revised manuscript; S.F.V. and D.E.V. approved final version of manuscript; M.P. prepared figures.

REFERENCES

1. **Asai K, Yang GP, Geng YJ, Takagi G, Bishop S, Ishikawa Y, Shannon RP, Wagner TE, Vatner DE, Homcy CJ, Vatner SF.** Beta-adrenergic receptor blockade arrests myocyte damage and preserves cardiac function in the transgenic G(salpha) mouse. *J Clin Invest* 104: 551–558, 1999.
2. **Bauman AL, Soughayer J, Nguyen BT, Willoughby D, Carnegie GK, Wong W, Hoshi N, Langeberg LK, Cooper DM, Dessauer CW, Scott JD.** Dynamic regulation of cAMP synthesis through anchored PKA-adenylyl cyclase V/VI complexes. *Mol Cell* 23: 925–931, 2006.
3. **Bourajjaj M, Armand AS, da Costa Martins P.A, Weijts B, van der Nagel R, Heeneman S, Wehrens XH, De Windt LJ.** NFATc2 is a necessary mediator of calcineurin-dependent cardiac hypertrophy and heart failure. *J Biol Chem* 283: 22295–22303, 2008.
4. **Bristow MR, Ginsburg R, Minobe W, Cubicciotti RS, Sageman WS, Lurie K, Billingham ME, Harrison DC, Stinson EB.** Decreased catecholamine sensitivity and beta-adrenergic-receptor density in failing human hearts. *N Engl J Med* 307: 205–211, 1982.
5. **Canto C, Auwerx J.** Caloric restriction, SIRT1 and longevity. *Trends Endocrinol Metab* 20: 325–331, 2009.
6. **Cao J, Sodhi K, Puri N, Monu SR, Rezzani R, Abraham NG.** High fat diet enhances cardiac abnormalities in SHR rats: protective role of heme oxygenase-adiponectin axis. *Diabetol Metab Syndr* 3: 37, 2011.
7. **CIBIS Investigators and Committees.** A randomized trial of beta-blockade in heart failure. The Cardiac Insufficiency Bisoprolol Study (CIBIS). *Circulation* 90: 1765–1773, 1994.
8. **CIBIS-II Investigators and Committees.** The Cardiac Insufficiency Bisoprolol Study I.I. (CIBIS-II): a randomized trial. *Lancet* 353: 9–13, 1999.
9. **Defer N, Best-Belpomme M, Hanoune J.** Tissue specificity and physiological relevance of various isoforms of adenylyl cyclase. *Am J Physiol Renal Physiol* 279: F400–F416, 2000.
10. **Dessauer CW, Gilman AG.** The catalytic mechanism of mammalian adenylyl cyclase. Equilibrium binding and kinetic analysis of P-site inhibition. *J Biol Chem* 272: 27787–27795, 1997.
11. **Du XJ, Gao XM, Wang B, Jennings GL, Woodcock EA, Dart AM.** Age-dependent cardiomyopathy and heart failure phenotype in mice over-